JOURNAL OF BACTERIOLOGY, July 2006, p. 4903–4917 Vol. 188, No. 13
0021-9193/06/$08.00+0 doi:10.1128/JB.00180-06

PopF1 and PopF2, Two Proteins Secreted by the Type III Protein Secretion System of *Ralstonia solanacearum*, Are Translocators Belonging to the HrpF/NopX Family†

Damien Meyer,[1] Sébastien Cunnac,[1]‡ Mareva Guéneron,[1]§ Céline Declercq,[1]¶ Frédérique Van Gijsegem,[2] Emmanuelle Lauber,[1] Christian Boucher,[1] and Matthieu Arlat[1]*

Laboratoire des Interactions Plantes-Microorganismes, INRA-CNRS, BP52627, 31326 Castanet tolosan Cedex,[1] and UMR INRA, INA-PG, Université Paris VI, Interactions Plantes Pathogènes, INA-PG, 16 rue Claude Bernard, 75231 Paris Cedex 05,[2] France

Received 3 February 2006/Accepted 14 April 2006

***Ralstonia solanacearum* GMI1000 is a gram-negative plant pathogen which contains an *hrp* gene cluster which codes for a type III protein secretion system (TTSS). We identified two novel Hrp-secreted proteins, called PopF1 and PopF2, which display similarity to one another and to putative TTSS translocators, HrpF and NopX, from *Xanthomonas* spp. and rhizobia, respectively. They also show similarities with TTSS translocators of the YopB family from animal-pathogenic bacteria. Both *popF1* and *popF2* belong to the HrpB regulon and are required for the interaction with plants, but PopF1 seems to play a more important role in virulence and hypersensitive response (HR) elicitation than PopF2 under our experimental conditions. PopF1 and PopF2 are not necessary for the secretion of effector proteins, but they are required for the translocation of AvrA avirulence protein into tobacco cells. We conclude that PopF1 and PopF2 are type III translocators belonging to the HrpF/NopX family. The *hrpF* gene of *Xanthomonas campestris* pv. *campestris* partially restored HR-inducing ability to *popF1 popF2* mutants of *R. solanacearum*, suggesting that translocators of *R. solanacearum* and *Xanthomonas* are functionally conserved. Finally, *R. solanacearum* strain UW551, which does not belong to the same phylotype as GMI1000, also possesses two putative translocator proteins. However, although one of these proteins is clearly related to PopF1 and PopF2, the other seems to be different and related to NopX proteins, thus showing that translocators might be variable in *R. solanacearum*.**

Ralstonia solanacearum is a soilborne bacterium that causes bacterial wilt disease in more than 200 plant species, including several economically important crops (30). Strain GM1000, whose complete genome sequence is known (64), is pathogenic on several solanaceous plants, such as tomato, pepper, eggplant, and petunia. On tobacco, this strain induces a typical defense reaction, called the hypersensitive response (HR), which is associated with resistance and is characterized by a rapid, localized programmed cell death of plant cells (53). Strain GMI1000 possesses a type III protein secretion system (TTSS) which controls both the ability to induce disease on host plants and to elicit the HR on tobacco. Components of this TTSS are encoded by a gene cluster, named the *hrp* (HR and pathogenicity) gene cluster, which comprises more than 20 genes and which is located on a megaplasmid (26).

hrp gene clusters have also been identified in other gram-negative plant pathogenic bacteria, such as *Xanthomonas* sp., *Erwinia* sp., *Pantoea stewartii*, and *Pseudomonas syringae* (1). Eleven *hrp* genes, renamed *hrc* genes, are conserved in all of these clusters, suggesting that they form the core of the Hrp TTSS secretion machinery (7). Two lineages of *hrp* gene clusters have been identified on the basis of *hrp* gene similarities and cluster organization: group I includes *Erwinia* sp., *Pantoea stewartii*, and *Pseudomonas syringae*, while group II includes *Xanthomonas* sp. and *R. solanacearum* (1, 27, 31).

Besides their conservation in phytopathogenic bacteria, TTSSs have also been found in a wide variety of gram-negative bacteria interacting with animals or insects as pathogens or as symbionts (18, 31). The key denominator explaining the wide conservation of these TTSSs certainly resides in the fact that they control the development of machineries capable of delivering proteins into the cytosol of eukaryotic cells (18, 31). Two classes of proteins are believed to be secreted by TTSSs: effectors that are translocated inside host cells and helper or accessory proteins that support the translocation of effectors (17, 56). Altogether, over 100 effectors or candidate effector genes have been identified in plant-pathogenic bacteria (2, 15, 21, 58). These effectors have a dual role (2). They are believed to control disease progression by countering plant defenses or by inducing nutrient release from the host cell. However, in some cases effectors trigger HR defense responses upon recognition by specific plant surveillance systems involving resistance (R) genes. In these cases, effectors are named avirulence (Avr) proteins, since they prevent pathogenicity on host plants containing a corresponding R gene (39).

TTSSs have been extensively analyzed in animal pathogens (18, 31). Their structure resembles the flagellar basal body, and

* Corresponding author. Mailing address: Laboratoire des Interactions Plantes-Microorganismes, INRA-CNRS, BP52627, 31326 Castanet tolosan Cedex, France. Phone: (33) 561 28 50 47. Fax: (33) 561 28 50 47. E-mail: arlat@toulouse.inra.fr.

† Supplemental material for this article may be found at http://jb.asm.org/.

‡ Present address: Department of Biological Sciences, Stanford University, Stanford, CA 94305-5020.

§ Present address: Protisvalor, Jardin du Pharo, 13007 Marseille, France.

¶ Present address: Plate-forme Transcriptome–Biopuces, Centre de Bioingenierie Gilbert Durand, Département de Génie Biochimique et Alimentaire, Institut National des Sciences Appliquées, 31077 Toulouse Cedex 4, France.

they are associated with an extracellular needle complex, which might function as a conduit for the transport of effector and accessory proteins. In plant pathogens, extracellular appendages associated with TTSSs have also been found (60). These so-called Hrp pili are much longer (several micrometers) than needle complexes, but they have the same diameter (~8 nm) (31). They are thought to penetrate the plant cell wall, which represents a major obstacle for the translocation process. Hrp pili have been described for *P. syringae*, *R. solanacearum*, and *Erwinia amylovora* (37, 59, 74) and more recently for *Sinorhizobium fredii*, *Rhizobium* sp. strain NGR234, and *Xanthomonas campestris* pv. *vesicatoria* (43, 63, 76). Mutations in genes encoding Hrp pili prevent secretion of effectors and other accessory proteins in vitro (31). This result and elegant immunogold labeling observations suggest that the Hrp pili appendages form a channel allowing protein transport across the plant cell wall (36, 49). However, needle complexes and Hrp pili are not sufficient to deliver proteins inside animal or plant cells. Other accessory proteins that interact with host membranes are necessary. In *Yersinia* TTSS, three accessory proteins, LcrV, YopB, and YopD, called translocators, seem to associate to form a translocon required for the translocation of effector proteins across the plasma membrane into mammalian host cells (16, 29, 33, 52, 65). The existence of translocators has also been proposed in phytopathogenic bacteria. HrpF of *Xanthomonas campestris* pv. *vesicatoria* is required for translocation of AvrBs3 or AvrBS2 effector proteins into the plant cell but not for their secretion in the extracellular medium (14, 61, 69). Moreover, HrpF can form pores in a planar lipid bilayer system (12); this protein may thus act as a translocator. HrpF displays similarity to NolX (recently renamed NopX [63]), a TTSS-secreted protein of *S. fredii* and *Rhizobium* sp. strain NGR234 (34, 42, 51). However, the possible role of NopX as a translocator has not yet been studied. More recently the HrpK protein, secreted via the *Pseudomonas syringae* pv. *tomato* strain DC3000 TTSS and which displays a weak homology with HrpF, was shown to be involved in protein translocation and might therefore be a putative translocator (56).

Recently, using genomic and functional approaches, five candidate effectors of strain GMI1000 were shown to be translocated into host-plant cells via the *R. solanacearum* TTSS (21). Although an Hrp pilus has been characterized in *R. solanacearum* (74), translocators have not yet been identified. Here we report the identification of two proteins, PopF1 and PopF2, which are secreted via the GMI1000 TTSS. These proteins display homology to one another and to HrpF and NopX, and we present evidence that they are translocators for the *R. solanacearum* TTSS. We also show that double mutants carrying mutations in *popF1* and *popF2* can be partially complemented by HrpF from *X. campestris* pv. *campestris*. The contributions of PopF1 and PopF2 to virulence and translocation differs. PopF1 plays a more important role in virulence and HR elicitation than PopF2 under our experimental conditions. These differences might be due to differences in amino acid (aa) sequences and/or expression levels.

MATERIALS AND METHODS

Bacterial strains, plasmids, and growth conditions. The bacterial strains and plasmids used for this study are described in Table 1. *Escherichia coli* cells were grown in Luria-Bertani medium at 37°C. *R. solanacearum* was grown at 28°C in complete medium B (8) or minimal medium supplemented with 20 mM glutamate (MMG) (5). When indicated, MMG was complemented with Congo red (100 μg ml^{-1}). *Xanthomonas campestris* pv. *campestris* cells were grown at 28°C in Kado's medium (5). Antibiotics were used at the following concentrations (in milligrams $liter^{-1}$): tetracyclin (Tc), 10 (*E. coli* and *R. solanacearum*) and 5 (*X. campestris* pv. *campestris*); ampicillin (Amp), 50; rifampin (Rif), 50; spectinomycin (Sp) 40; streptomycin (Sm) 200; kanamycin (Km) 25; gentamicin (Gm) 10 (*E. coli*) and 20 (*R. solanacearum*); and chloramphenicol (Cm), 12.5.

Bacterial conjugation, electroporation, and transformation. Conjugations and triparental matings were performed as described previously by Arlat and colleagues to introduce plasmids into *R. solanacearum* (4) or *X. campestris* pv. *campestris* (3). Plasmids were also introduced into *R. solanacearum* strains by electroporation as previously described (46). Transformation of strains of *R. solanacearum* leading to homologous recombination of the incoming DNA was performed according to the method of Boucher et al. (8).

Molecular biology techniques, DNA sequencing, and sequence analysis. Standard recombinant DNA techniques were performed as described previously (6). Chromosomal DNA was extracted from *R. solanacearum* or *X. campestris* pv. *campestris* as previously described (4). Restriction enzymes, DNA ligase, *Taq* polymerase (Invitrogen), and other DNA enzymes were used according to the manufacturer's recommendations. PCR amplifications were done in 50-μl volumes using genomic DNA of *R. solanacearum* strain GMI1000 or *X. campestris* pv. *campestris* strain 8004 (73). Sequences of oligonucleotide primers are listed in Table S1 in the supplemental material. To sequence the *X. campestris* pv. *campestris* 8004 *hrpF* gene and to verify junctions of all the constructs, including the His_6 epitope fusion constructs, double-stranded plasmid templates were sequenced automatically with a Perkin Elmer/ABI3700 Sequencer.

DNA and protein sequences were analyzed using the GCG software package (Wisconsin Package version 9.0; Genetics Computer Group) or the Vector NTI package. Homology searches were performed using the NCBI BLAST server. The putative terminator sequences were found using the GCG program terminator.

Phylogenetic analyses. Amino acid sequences were aligned and phylogenetic trees were reconstructed by the neighbor-joining method as implemented in ClustalX (71).

β-Galactosidase assays. After collecting the bacteria by centrifugation and resuspending the pellet in water, the β-galactosidase activity was measured as described previously (4).

Cloning the *hrpF* gene of *X. campestris* pv. *campestris* strain 8004. A 3.5-kb DNA fragment containing the *hrpF* gene sequences and promoter region (757 bp upstream of the ATG codon) was PCR amplified using primers PFXcc1 and FFXcc2 and cloned into the pGEM-T vector, giving plasmid pMD1. The cloned DNA fragment was sequenced using PFXcc1 and FFXcc2 primers and additional internal primers HS-10, HR-6, FS-2, FR-2 HR-4bis, and HS. The sequence of this DNA fragment matches, with 98% identity, the corresponding sequence of *X. campestris* pv. *campestris* strain ATCC33913 (22) (from nucleotides 1423578 to 1427109). The HrpF protein deduced from the 8004 strain is 99% identical to HrpF from strain ATCC33913. Plasmid pMD1 was double digested by HindIII and EcoRI to subclone the *hrpF* sequence into the pLAFR6 polylinker (35), generating plasmid pHrpF.

Cloning of the *popF1* and *popF2* genes. A 2,506-bp DNA fragment containing the *popF1* gene sequences and the 317-bp DNA region located immediately upstream of the *popF1* start codon was PCR amplified using GMI1000 genomic DNA as a template and primers POPF1H and POPF1X. This fragment was cloned into the pCZ367 plasmid. The HindIII-KpnI fragment carried by this new construct was then subcloned into pLAFR6, generating plasmid pPopF1 (see Fig. 3B). A very similar strategy was used to clone the *popF2* gene into pLAFR6. Primers POPF2H and POPF2X were used to amplify a 2,486-bp fragment using GMI1000 DNA as a template. This DNA fragment, which carries *popF2* coding sequences and the upstream DNA region (265 bp), was cloned into pCZ367 and subcloned into pLAFR6 after HindIII/KpnI digestion, thus generating the pPopF2 plasmid (see Fig. 3B).

Construction of *popF1* and *popF2* promoter-reporter plasmids. The *popF1* promoter region (600 bp), corresponding to positions −601 to −1 relative to the A nucleotide of the *popF1* start codon, was PCR amplified using primers HINDF1 and PF1X and cloned into the pGEM-T vector. The HindIII and XbaI restriction sites carried by HINDF1 and PF1X primers, respectively (boldface type in Table S1 in the supplemental material), were used to clone this fragment into the pCZ205 vector, which contains the *lacZ* gene sequences without a promoter. This construct, named pCZ406, was digested by HindIII and KpnI, generating a 4.6-kb DNA fragment carrying the *popF1* promoter region, *lacZ* coding sequence, and a gene coding for gentamicin resistance. This fragment was

TABLE 1. Bacterial strains and plasmids used in this study

Strain or plasmid	Relevant genotype or characteristics	Source or reference
Strains		
E. coli DH5α	F⁻ *recA lacZ*ΔM15	BRL
R. solanacearum		
GMI1000	Wild-type strain	8
GMI1402	*hrcS*::Tn*5*-B20 mutant	4
GMI1410	*hrpY*::Tn*5*-B20 mutant	4
GMI1475	*hrpB*::Tn*5*-B20 mutant	4
GMI1551	*PopA*::$\Omega_{Sp/Sm}$	5
GMI1575	*prhA*::Ω mutant	50
GMI1663	*popF1*::$\Omega_{Sp/Sm}$ mutant	This study
GMI1664	*popF2*::Ω_{Cm} mutant	This study
GMI1665	*popF2*:: *aprA* (Gm) mutant	This study
GMI1666	*popF1*::$\Omega_{Sp/Sm}$ *popF2*::Ω_{Cm} double mutant	This study
GMI1667	*popF1*::$\Omega_{Sp/Sm}$ *popF2*::*aprA* (Gm^r) double mutant	This study
GMI1668	*popF2*-His_6, Sp^r/Sm^r	This study
GMI1669	*popF2*-His_6 *hrcS*::Tn*5*-B20, Sp^r/Sm^r Km^r	This study
GMI1670	*popF2*-His_6 (Sp/Sm) *hrpY*::Tn*5*-B20, Sp^r/Sm^r Km^r	This study
X. campestris pv. *campestris* 8004	Wild type, Rif^r	73
Plasmids		
pBluescript II KS(−)	Cloning vector, Amp^r	Stratagene
pGEM-T	Cloning vector, Amp^r	Promega
pHP45Ω $_{Sp/Sm}$	Sp^r, Sm^r, Ω cassette	57
pHP45Ω_{Cm}	Cm^r, Ω cassette	57
pLAFR6	Tc^r	35
pMS107	pIC20H containing the *cyaA* gene	67
pUC1318 Apra/Gm	Gm^r, *aprA* cassette	9
pAM5	pLAFR3 with a 2-kb insert containing *hrpB*, Tc^r	28
pCL1	pGEM T with a 2.5-kb insert containing *popF2*, Amp^r	This study
pCL3	pGEM-T with a 1.5-kb fragment containing *popF1* N-terminal DNA region, Amp^r	This study
pMG6	pBluescript KS(−) with a 1-kb XbaI HindIII fragment containing *popF2* C-terminal DNA region, Amp^r	This study
pCL86	pCZ205 with a 712-bp HindIII XbaI fragment carrying *popF2* promoter, Amp^r Gm^r	This study
pCL94	pLAFR6 carrying a 4.7-kb fragment carrying *popF2* promoter and promoterless *lacZ*, Tc^r Gm^r	This study
pCZ205	pUC19 carrying *lacZ* in KpnI-XbaI, Amp^r Gm^r	46
pCZ367	pUC18-derived vector used for insertional mutagenesis, Amp^r Gm^r	21
pCZ406	pCZ205 with a 600-bp HindIII XbaI fragment carrying *popF1* promoter, Amp^r Gm^r	This study
pCZ408	pLAFR6 carrying a 4.6-kb fragment carrying *popF1* promoter and promoterless *lacZ*, Tc^r Gm^r	This study
pHrpF	pLAFR6 with a 3.5-kb HindIII-EcoRI fragment containing $hrpF_{Xcc}$, Tc^r	This study
pMG7	pMG6 with a 1-kb HindIII XhoI fragment containing *popF2* C-terminal DNA region, Amp^r	This study
pMDI	pGEM-T with a 3.5-kb HindIII-EcoRI fragment containing $HrpF_{Xcc}$, Amp^r	This study
pPopF1	pLAFR6 with a 2.5-kb HindIII-KpnI fragment carrying *popF1*	This study
pPopF2	pLAFR6 with a 2.5-kb HindIII-KpnI fragment carrying *popF1*	This study
pSC154	pET-26b(+)-derived vector with the *cyaA′* gene from pMS107 used for translational fusion constructs; the T7 promoter is replaced by a ptac promoter, Km^r	21
pSC163	PLAFR6 carrying a translational fusion between $avrA_{1-99}$ and *cyaA′*	19

cloned into pLAFR6 digested by HindIII and KpnI, thus generating the pCZ408 reporter plasmid (see Fig. 3B).

The promoter region of *popF2* was cloned into a pGEM-T vector after PCR amplification of a 712-bp DNA fragment spanning positions −712 to −1 relative to the A nucleotide of the ATG start codon. GMI1000 genomic DNA was used as a template for primers PF2H and PF2X, which contain HindIII or XbaI restriction sites, respectively (Table S1 in the supplemental material). The XbaI/HindIII fragment was then cloned into the pCZ205 vector, thus generating plasmid pCL86. This plasmid was digested by HindIII and KpnI, generating a 4.7-kb DNA fragment carrying the *popF2* promoter region, *lacZ* coding sequence, and a gene coding for gentamycin resistance, which was cloned into pLAFR6 digested by HindIII and KpnI, thus generating the pCL94 reporter plasmid (see Fig. 3B). pCL94 and pCZ408 were introduced in *R. solanacearum* strains by triparental matings.

Construction of *popF1* or *popF2* single mutants and *popF1 popF2* double mutants. The *popF1* gene was disrupted by insertion of the $\Omega_{Sp/Sm}$ interposon. A 1,570-bp DNA fragment, corresponding to position −213 to +1345 relative to the ATG start codon of *popF1*, was PCR amplified using primers MFD and MFB2 and cloned into pGEM-T, thus generating pCL3. This plasmid was linearized by EcoRI and ligated with an EcoRI-digested $\Omega_{Sp/Sm}$ interposon, generating plasmid pCL3::$\Omega_{Sp/Sm}$, which was then linearized by XbaI and used to transform various *R. solanacearum* strains. Transformants were selected on media containing spectinomycin and streptomycin.

The *popF2* gene was disrupted by insertion of the Ω_{Cm} interposon (57) or by insertion of the *aprA* cassette, which confers resistance to gentamicin (Gm^r) (9). A 2.4-kb DNA fragment, corresponding to positions −220 to +2211 relative to the ATG start codon of *popF2*, was PCR amplified using GMI1000 genomic DNA as template and primers MF2D and MF2F, which contain XbaI and

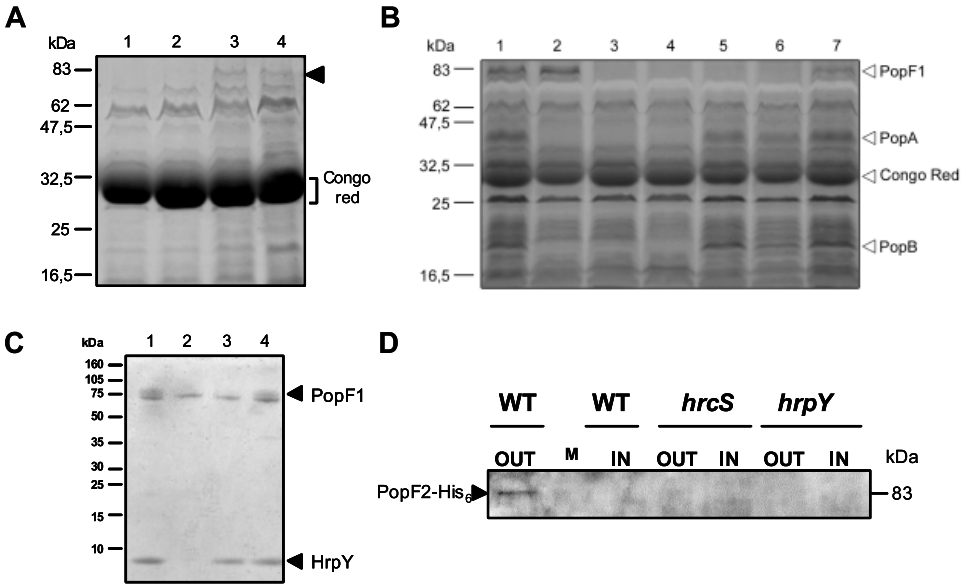

FIG. 1. Secretion of PopF1 and PopF2 and detection of PopF1 in Hrp pili preparations. (A) Protein secretion after growth of various *R. solanacearum* strains carrying pAM5 in the presence of Congo red. Proteins present in CSP-CRs prepared from (lane 1) *hrp* mutant strain GMI1410(*hrpY*)/pAM5, (lane 2) *hrp* mutant strain GMI1402(*hrcS*)/pAM5, (lane 3) GMI1551(*popA*)/pAM5, and (lane 4) GMI1000/pAM5 grown in MMG supplemented with Congo red were separated by SDS-PAGE and visualized by Coomassie blue staining. The arrowhead shows the new putative 80-kDa Hrp-secreted protein. The bracket indicates the position of Congo red, which in SDS-PAGE exhibits the same electrophoretic mobility as a 28-kDa protein. (B) Proteins present in CSP-CRs prepared from GMI1000/pAM5 (lane 1), GMI1551(*popA*)/pAM5 (lane 2), *hrp* mutant strain GMI1402(*hrcS*)/pAM5 (lane 3), GMI1410 (*hrpY*)/pAM5 (lane 4), GMI1663 (*popF1*)/pAM5 (lane 5), GMI1666 (*popF1 popF2*)/pAM5 (lane 6), and GMI1664 (*popF2*)/pAM5 (lane 7), grown in MMG supplemented with Congo red, were separated by SDS-PAGE and visualized by silver staining. Positions of PopA, PopB, PopF1, and Congo red are shown by arrowheads. (C) Characterization of PopF1 in Hrp pili preparations. Shown is a Tris-Tricine SDS-PAGE electrophoresis gel (10 to 20% acrylamide) loaded with protein samples prepared from the surface of the following strains grown on MMG: (lane 1) GMI1000, (lane 2) GMI1584(*hrcV*) mutant, (lane 3) GMI1663(*popF1*) mutant, and (lane 4) GMI1664(*popF2*) mutant. Proteins were revealed by Coomassie blue staining. Arrowheads show PopF1 and HrpY. (D) Secretion of PopF2-His$_6$ in wild-type (WT) or *hrp* background. Bacterial strains GMI1668(*popF2*-His$_6$), GMI1669(*hrcS popF2*-His$_6$), and GMI1670(*hrpY popF2*-His$_6$) were cultivated in MMG supplemented with Congo red. Concentrated supernatant preparations (CSP-CR) (OUT) and concentrated lysate preparations (CLP-CR) (IN) were prepared from these cultures, and their protein contents were separated by SDS-PAGE and visualized by immunoblotting with an anti-His$_6$ monoclonal antibody. M, size marker.

HindIII restriction sites, respectively (underlined in the primer sequences). This DNA fragment was cloned into pGEM-T, generating plasmid pCL1. This plasmid was linearized by BglII and then ligated with the Cm^r Ω_{Cm} interposon obtained by BamHI digestion of the plasmid pHP45Ω_{Cm}, thus generating plasmid pCL1::Ω_{Cm}. This plasmid was linearized by XbaI and used to transform various *R. solanacearum* strains. Transformants were selected on media containing chloramphenicol.

Alternatively, pCL1 was linearized by SmaI and ligated with the *aprA* cassette obtained by digestion of plasmid pUC1318 by SmaI. This new construct, named pCL1::*aprA*, was linearized by XbaI and used to transform various *R. solanacearum* strains. Transformants were selected on media containing gentamicin.

To obtain *popF1 popF2* double mutants, the *popF1*::$\Omega_{Sp/sm}$ mutant GMI1663 was transformed with plasmid pCL1::Ω_{Cm} or pCL1::*aprA* linearized by XbaI. Transformants were either selected on media containing spectinomycin and chloramphenicol or spectinomycin and gentamicin, thus generating mutants GMI1666 and GMI1667, respectively.

Gene replacements were checked by PCR and by Southern hybridizations.

Modifications of *popF2*. A DNA sequence encoding a His$_6$ epitope (HHHHHH) was added at the C terminus of *popF2* by PCR. For this purpose, GMI1000 genomic DNA was used to amplify the *popF2*-His$_6$ fusion gene using the primers CF2D and CF2F. Primer CF2D contains an XbaI restriction site (underlined in the primer sequence) followed by the sequence of 5 amino acid codons of *popF2* (codons 392 to 397); CF2F contains the sequence of the five carboxy-terminal amino acid codons of *popF2*, followed by the His$_6$ coding sequence, a stop codon, and a HindIII restriction site (in boldface type in the primer sequence). The PCR product was digested by XbaI and HindIII, and the 1,062-bp fragment was cloned into pBluescript KS(−), generating plasmid pMG6.

A 970-bp HindIII/XhoI fragment corresponding to the DNA sequence located immediately downstream of the *popF2* stop codon was generated by PCR amplification from GMI1000 genomic DNA using the primers PF2D and PF2F. After digestion by HindIII and XhoI (underlined in the PF2D and PF2F primer sequences, respectively), the PCR product was subcloned into pMG6 digested by HindIII and XhoI, producing plasmid pMG7. This plasmid was linearized by HindIII and then ligated with the Sm^r/Sp^r $\Omega_{Sp/Sm}$ interposon obtained by HindIII digestion of the plasmid pHP45$\Omega_{Sp/Sm}$ (57), giving pMG7::$\Omega_{Sp/Sm}$. This plasmid was then linearized by XbaI and used to transform strain GMI1000. Transformants were selected on media containing streptomycin and spectinomycin. Gene replacements were checked by Southern hybridization.

Detection of Pop proteins in the supernatant and cell lysate. Strain GMI1000 and derivatives were grown at 28°C for 16 h in MMG or MMG supplemented with Congo red (MMG-CR). Concentrated supernatant preparation (CSP or CSP-CR) and concentrated cell-free lysate (CLP) were prepared as described by Gueneron et al. (28) and analyzed by sodium dodecyl sulfate-polyacrylamide gel electrophoresis.

SDS-PAGE and immunoblotting. Electrophoresis of proteins in 12.5% polyacrylamide gels in the presence of sodium dodecyl sulfate (SDS-PAGE) was performed as described by Laemmli (45). After electrophoresis, proteins were either silver stained using the Silver Stain Plus kit (Bio-Rad, Calif.) or transferred onto a nitrocellulose membrane. Immunoblotting experiments were performed with rabbit polyclonal antibodies raised against PopA (data not shown) or with the mouse anti-His$_6$ monoclonal antibody (Roche Molecular Biochemicals, Germany) which allows the detection of His$_6$-tagged recombinant proteins. Peroxidase-conjugated sheep anti-mouse or goat anti-rabbit was used as secondary antibody and detected by using the ECL chemoluminescence kit (Amersham Pharmacia Biotech, Orsay, France).

Hrp pilus proteins. Bacterial cell exostructures were isolated as previously described in Van Gijsegem et al. (74). Bacteria were grown in MMG solid medium and were resuspended in 10 mM Tris-HCl, pH 8, buffer, and their exostructures were shaved off by passing the bacterial suspension several times

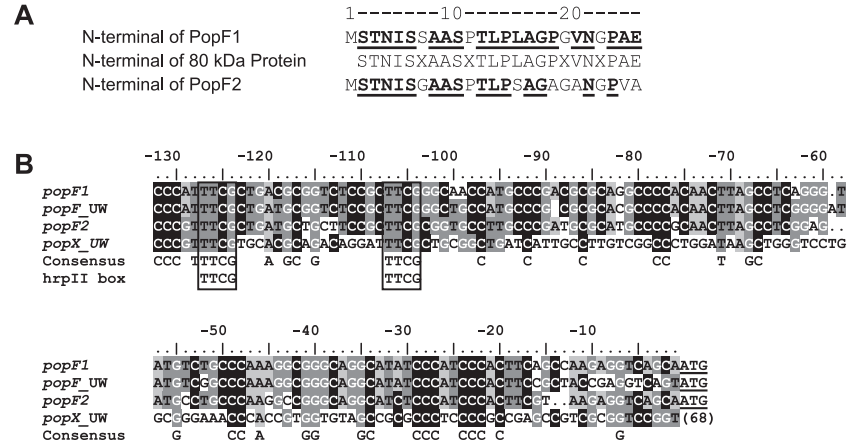

FIG. 2. Sequence alignments of PopF1 and PopF2 N-terminal regions and of promoter DNA regions of *popF1*, *popF2*, $popF_{UW551}$, and $popX_{UW551}$. (A) Sequence alignment of the N-terminal sequences of the putative 80-kDa Hrp-secreted proteins PopF1 and PopF2. Amino acids from PopF1 or PopF2 present in the N-terminal sequence of the 80-kDa Hrp-secreted protein are shown in boldface and underlined. The ruler on the top of the sequences indicates amino acid position in PopF1 and PopF2. X, unknown amino acid. (B) Sequence alignment of *popF1*, *popF2*, $popF_{UW551}$, and $popX_{UW551}$ promoters. Nucleotides that are highlighted at a given position in the alignment are conserved in at least 50% of the sequences. The underlined three final nucleotides of *popF1*, *popF2*, and $popF_{UW551}$ correspond to the initiation codon. The first adenine of this codon was used as the origin for the numbering of the sequence ruler. The number to the right of $popX_{UW551}$ sequences represents the distance from the initiation codon. The open boxes indicate the hrp_{II} box.

through a 28-gauge needle. Bacteria were then pelleted by centrifugation, and exostructures in the supernatant were partially purified by centrifugation in a Beckman SW40.1 swinging bucket rotor, first for 20 min at 6,000 × *g*. The supernatant was then collected and submitted to a subsequent 3-h centrifugation at 85,000 × *g*. The pellet containing the Hrp pili was resuspended in 10 mM Tris-HCl buffer and analyzed by SDS-PAGE using 10 to 20% Tris-Tricine Ready gels (Bio-Rad).

Protein sequencing. After SDS-PAGE electrophoresis, proteins present in the CSP-CR of the wild-type strain GMI1000 were transferred onto polyvinylidene difluoride (PVDF) membranes (Problott Applied Biosystem). Protein bands on PVDF membranes were detected by Amido Black staining (N-3393; Naphtol Blue Black; Sigma). The 80-kDa protein band was cut out and microsequenced.

Automated Edman degradation of proteins was performed using an Applied Biosystems 475A sequencer and its online phenylthiohydantoin amino acid analyzer (model 120A); the reagents and methods were as specified by the manufacturer (Applied Biosystems, Roissy, France).

SDS-PAGE and immunodetection of $AvrA_{1-99}$::CyaA fusion protein. The construction of the $avrA_{1-99}$::*cyaA* gene fusion has been described in detail by Cunnac (19). Briefly, a DNA fragment corresponding to codons 1 to 99 of *avrA* was generated by PCR amplification using GMI1000 DNA as a template and primers AvrA1 and AvrA2. This fragment was cloned into plasmid pSC154 to generate a translational fusion between $AvrA_{1-99}$ and the CyaA′ coding sequences. The fusion construct was then subcloned into pLAFR6, generating plasmid pSC163. Immunodetection of CyaA fusion proteins was conducted as previously described by Cunnac et al. (21).

Adenylate cyclase (CyaA) translocation assay. The procedures for adenylate cyclase assay were previously described in Schechter et al. (66) and in Cunnac et al. (21).

GMI1000 strain and derivatives carrying plasmid pSC163 were infiltrated into *Nicotiana benthamania* leaves at an optical density of 1.0 (21). Plants were sampled 7 h later with a cork borer. Leaf disks were transferred into Eppendorf tubes and immediately frozen in liquid nitrogen. For cyclic AMP (cAMP) extraction, samples in Eppendorf tubes were kept frozen while grinding by shaking with 2-mm tungsten beads shaken in a QIAGEN Mixer Mill MM300 for two runs of 2 min at 30 Hz. Samples were stored at −80°C before cAMP quantitation. Protein concentration was assessed with the Bio-Rad protein assay kit. Cyclic AMP (cAMP) levels were monitored with a cAMP enzyme immunoassay kit (Biotrak; Amersham Pharmacia Biotech) according to the manufacturer's instructions.

Plant tests. HR tests on tobacco leaves and pathogenicity assays on tomato plants were performed as previously described (50).

RESULTS

Characterization of *popF1* and *popF2*, two genes encoding novel putative Hrp-secreted proteins. In a previous study we compared, by SDS-PAGE and silver staining analysis, concentrated supernatant preparations (CSPs) of strain GMI1000 and *hrp* mutants carrying pAM5, a plasmid harboring the *hrpB* regulatory gene which allows overexpression of *hrp* genes. After growth in minimal medium supplemented with Congo red (CSP-CR), this work allowed the detection of PopB and of four additional putative Hrp-secreted proteins (28). Among these proteins, we identified an ~80-kDa protein which was also present in CSP-CRs of mutants altered in the *popABC* operon, suggesting that it might correspond to a novel Hrp-secreted protein. Interestingly, this band (apparent M_r, 80,000) was also detectable by SDS-PAGE and Coomassie blue staining analysis in CSPs or CSP-CRs of the wild-type strain carrying pAM5, but it was never visible in CSPs or CSP-CR of *hrp* mutants harboring pAM5 (Fig. 1). Amino-terminal sequencing of the putative 80-kDa Hrp-secreted protein gave a 24-amino-acid sequence with 4 ambiguous residues (Fig. 2). This N-terminal sequence was used as a query and compared with sequences in the protein database deduced from the annotation of the complete genome sequence of strain GMI1000 (http://bioinfo.genopole-toulouse.prd.fr/annotation/iANT/bacteria/ralsto/). This allowed the identification of two genes, RSp0900 and RSp1555, coding for proteins that match the 24-amino-acid (aa) query sequence. Whereas the amino acid sequence of residues 2 to 25 of the putative protein encoded by gene RSp1555 matched the N-terminal amino acid sequence of the 80-kDa protein exactly (Fig. 2), that of the protein deduced from the RSp0900 gene matched the 24-aa query sequence partially. The RSp1555 and RSp0900 genes were subsequently named *popF1* and *popF2*, respectively. Both genes are located on the megaplasmid of strain GMI1000; *popF2* maps approx-

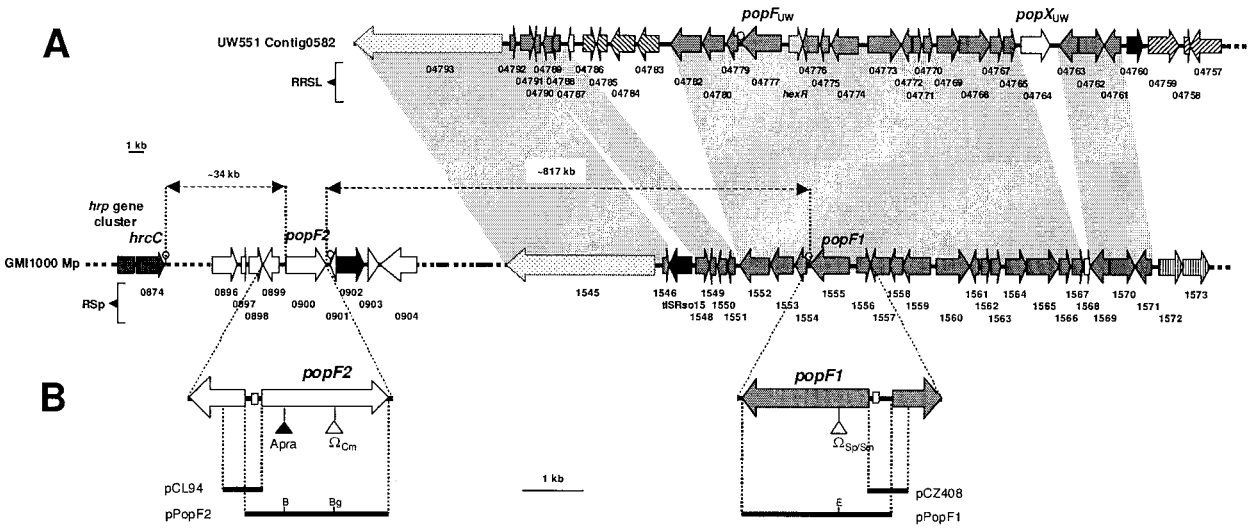

FIG. 3. Genetic organization and relationships between genomic regions encompassing *popF1* and *popF2* in strain GMI1000 and $popF_{UW551}$ and $popX_{UW551}$ in strain UW551. (A) Representation of a GMI1000 megaplasmid (Mp) DNA region located at the righthand end of the *hrp* gene cluster and encompassing *popF1* and *popF2* (top) as well as genetic organization of part of contig0582 (accession no. NZ_AAKL01000001) of the strain UW551 draft genome sequence, which contains $popF_{UW551}$ and $popX_{UW551}$. Big arrows represent the predicted protein-coding genes. Arrows filled in dark gray correspond to orthologous genes having the same relative position in both strains. Hatched arrows represent genes having orthologs in the genome of the other strain but at different sites. A light gray arrow corresponds to *hexR* in UW551, which is present in strain GMI1000 (Rsp1556) and was not annotated in UW551. The dotted arrows represent Rsp1545 and RRSL04793 ORFs that display significant homologies but might not be true orthologs (data not shown). Putative integrase/recombinase or transposase genes are represented by black arrows. White arrows correspond to ORFs unique to each strain. Open circles show the position of putative Rho-independent transcription terminators. Colinear regions are shown by gray boxes. (B) Mutations and plasmids. The *popF1* and *popF2* DNA regions have been enlarged. Triangles show Ω or *aprA* cassette insertion sites. Horizontal black bars indicate sequences used in plasmid constructions. B, BamHI; Bg, BglII; E, EcoRI.

imately 34 kb to the right-hand side of the *hrp* gene cluster, whereas *popF1* lies ~817 kb to the right of *popF2* (Fig. 3A). The *popF2* and *popF1* genes seem to be surrounded by genes that have no apparent direct relationship with the TTSS.

PopF1 and PopF2 belong to the HrpF/NopX family. *popF1* and *popF2* code for putative proteins of 726 and 736 amino acids, with molecular masses of 77.28 and 78.08 kDa, respectively. These calculated molecular masses are in agreement with the apparent size of the sequenced protein. The theoretical pIs of PopF1 and PopF2 are significantly different, since that of PopF1 is 5.82 whereas that of PopF2 is 7.14.

The amino acid sequences of PopF1 and PopF2 share significant homology to one another, with 81% identity and 86% similarity (Table S2 in the supplemental material). Compared with sequences in the databases using BlastP, both PopF1 and PopF2 showed significant homology with the putative HrpF translocator from *Xanthomonas campestris* pv. *vesicatoria* and other *Xanthomonas* species or pathovars. Significant homologies were also observed with NopX from the symbiotic rhizobia *S. fredii*, *Rhizobium* sp. strain NGR234, and *Mesorhizobium loti*, which are related to HrpF (11). A summary of these results is presented in Fig. 4 and in Table S2 in the supplemental material.

Characterization of PopF1 and PopF2 homologs in *R. solanacearum* strain UW551. In fact, PopF1 and PopF2 showed the most significant similarities with RRSL_04777 protein from *R. solanacearum* strain UW551, for which a draft genome was recently obtained and annotated (25). Both proteins also displayed similarities with another protein of strain UW551, named RRSL_04764 (Table S2 in the supplemental material). RRSL_04777 displayed the best homologies with PopF2 (81% identity, 89% similarity) and PopF1 (78% identity, 85% similarity), whereas RRSL_04764 showed the best homologies with NopX from *S. fredii* and *Rhizobium* sp. strain NGR234 (63% identity, 77% similarity). The level of homology of RRSL_04764 with PopF1, PopF2, and RRSL_04777 was significantly lower (Table S2 in the supplemental material). RRSL_04777 and RRSL_04764 were subsequently named $PopF_{UW551}$ and $PopX_{UW551}$, respectively. It is worth noting that the theoretical pIs of $PopF_{UW551}$ and $PopX_{UW551}$ are both acidic, with values of 5.73 and 4.62, respectively. $popF_{UW551}$ and $popX_{UW551}$ genes are located on the same contig (Cont0582, accession no. NZ_AAKL01000001) (Fig. 3A). $popF_{UW551}$ is surrounded by genes orthologous to those bordering *popF1* in strain GMI1000, whereas $popX_{UW551}$, which has no direct homolog in GMI1000, maps between two open reading frames (ORFs) which have orthologs in strain GMI1000. Interestingly these two GMI1000 orthologous ORFs border ORF RSp1568, which has no ortholog in the UW551 genome (Fig. 3A). The *popF2* gene is located in a region which seems to be absent in strain UW551 (Fig. 3A). Therefore, it appears that, as observed for strain GMI1000, there are two genes coding for putative TTSS translocators in UW551. However, if one gene, $popF_{UW551}$, seems to be well conserved with those of GMI1000, the other one, $popX_{UW551}$, seems to be different (see below).

PopF and HrpF proteins display similarities to animal pathogen translocators of the YopB family and to HrpK translocator of *P. syringae*. PopF1, PopF2, and $PopF_{UW551}$ also

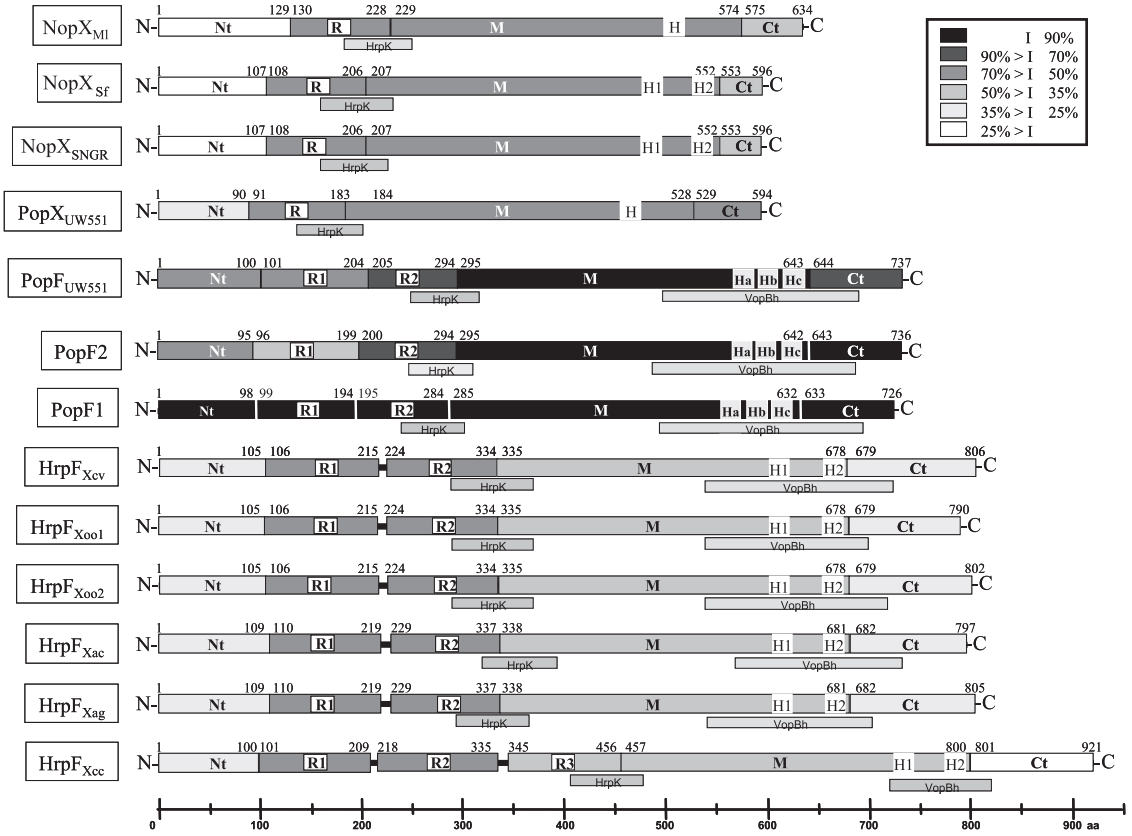

FIG. 4. Schematic diagram of the structural organization and homologies between the HrpF, NopX, and PopF proteins. Proteins are shown by boxes and are subdivided into domains Nt, R, M, and Ct. Numbers located above each protein correspond to amino acid positions relative to their initiation codon and show domain borders. The level of identity (I) of each protein domain with the equivalent domain of PopF1 is presented with a black/gray color code. Putative transmembrane regions (H) are represented by gray boxes with white borders. Regions with homologies to HrpK or VopBh are indicated by adjacent gray bars (HrpK, *Pseudomonas syringae* pv. *tomato* DC3000, accession no. AAF771489; VopBh, *Vibrio harveyi*, accession no. AAS13307). Shown are *Ralstonia solanacearum* PopF1 (accession no. NP_523114); PopF2 (accession no. NP_522461); strain UW551 PopF$_{UW551}$ (accession no. EAP74907) and PopX$_{UW551}$ (accession no. EAP74895); *Mesorhizobium loti* NopX (NopX$_{Ml}$; accession no. NP_106860); *Sinorhizobium fredii* NopX (NopX$_{Sf}$; accession no. AAB19229); *Rhizobium* NGR234 NopX (NopX$_{NGR}$; accession no. AAB91942); *Xanthomonas campestris* pv. *vesicatoria* HrpF (HrpF$_{Xcv}$; accession no. AAB86527); *Xanthomonas oryzae* pv. *oryzae* strain MA311018 HrpF (HrpF$_{Xoo1}$; accession no. BAB07869); *X. oryzae* pv. *oryzae* PXO99A HrpF (HrpF$_{Xoo2}$; accession no. AAS48653); *Xanthomonas axonopodis* pv. *citri* HrpF (HrpF$_{Xac}$; accession no. NP_640749); *X. axonopodis* pv. *glycines* HrpF (HrpF$_{Xag}$; accession no. AAP34358); *X. campestris* pv. *campestris* HrpF (HrpF$_{Xcc}$; accession no. NP_636591).

display some degree of similarity with putative translocators from animal pathogens related to YopB of *Yersinia* spp. The highest score was obtained with VopB from *Vibrio harveyi* (VopB$_{Vh}$), which is part of the TTSS of this marine pathogen (32). The similarity was restricted to an ~200-aa region located at the C terminus of PopF proteins (Fig. 4; Table S2 in the supplemental material). Other homologous proteins of this family include AopB from *Aeromonas hydrophila* (77), PopB from *Pseudomonas aeruginosa* (24), and YopB from *Yersinia enterocolitica*, *Yersinia pseudotuberculosis*, or *Yersinia pestis* (16), which gave less significant scores (Table S2 in the supplemental material). A multiple alignment between representatives of the YopB translocator family and the homologous sequence of PopF1 showed that the similarity occurs in one of the most conserved regions among YopB family members (Fig. 5). A BlastP search queried with the VopB$_{Vh}$ region (aa 113 to 319) displaying homology to PopF1 and PopF2 showed that this region is also conserved in *Xanthomonas* HrpF proteins (*E* values ranging from 6e-4 to 7.6e-1) but not significantly in PopX$_{UW551}$ or in *Rhizobia* NopX proteins (Fig. 4).

Recently, using the PSI-BLAST program, Petnicki-Ocwieja et al. (56) showed that HrpK, a putative translocator of *P. syringae* pv. *tomato* TTSS, is similar to HrpF, NopX, PopF1, and PopF2 proteins over a 97-aa region located in the central part of these proteins (Fig. 4). This region is very well conserved among NopX, HrpF, PopF1, PopF$_{UW551}$, and PopX$_{UW551}$ proteins, but it is less conserved in PopF2.

Altogether, these similarities with the YopB family and with HrpK suggest that PopF1 and PopF2 are putative type III translocators of *R. solanacearum* strain GMI1000.

PopF1 and PopF2 contain putative transmembrane domains. HrpF and HrpK proteins are known to share common structural features, such as transmembrane domains (TM), with the *Yersinia* YopB translocator and other translocators from animal pathogens (11, 56). Two putative TM domains, named H1 and H2, have been characterized in HrpF of *X.*

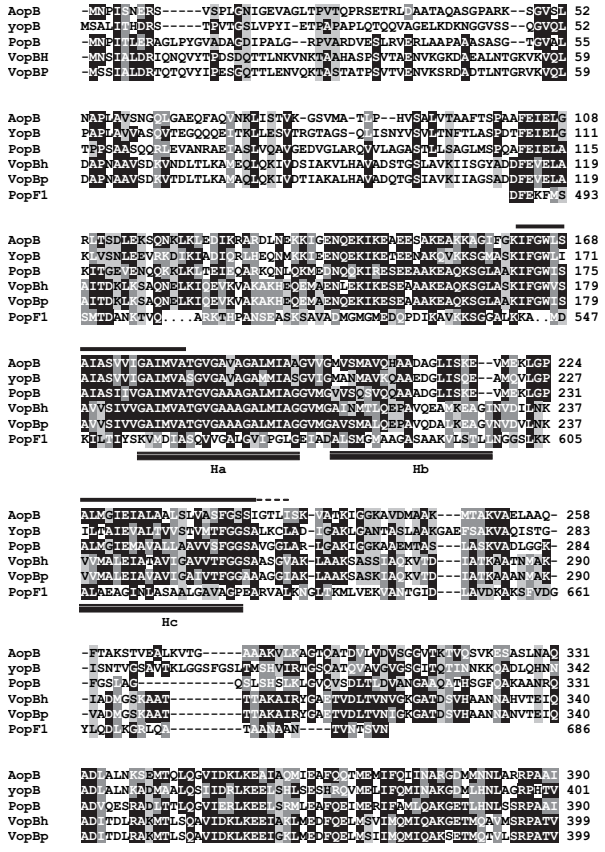

FIG. 5. Amino acid sequence alignment of the region within PopF1 that is similar to YopB homologues. The PopF1 amino acid sequence from aa 487 to aa 686 was aligned with YopB from *Yersinia enterolitica* (accession no. AAD16813) and related TTSS putative translocators: AopB from *Aeromonas hydrophila* (accession no. AAS91821), PopB from *Pseudomonas aeruginosa* PAO1 (accession no. NP_250399), VopBh from *Vibrio harveyi* (accession no. AAS13307), and VopBp from *Vibrio parahaemolyticus* (accession no. NP_798036). Black boxes correspond to identical amino acids or conserved residues present in at least 50% of the sequences, dark gray indicates conserved substitutions, and light gray indicates semiconserved substitutions (following the ClustalW alignment sequence criteria [72]). Bars above the sequence of AopB represent the putative TM helices identified in YopB family proteins. The dashed line corresponds to a TM extension in YopB, PopB, VopBh, and VopBp. Double bars below the sequence of PopF1 show the position of Ha, Hb, and Hc putative TM of this protein. The ClustalW program was used for protein alignment.

campestris pv. *vesicatoria* (hereafter named $HrpF_{Xcv}$) and NopX of *Rhizobium* sp. NGR234 (hereafter named NGR234 and $NopX_{NGR}$) (11, 34) (Fig. 4).

We used the TMpred program (http://www.ch.embnet.org/software/TMPRED_form.html) to identify putative TM segments in PopF1 and PopF2 and in related proteins. Three hydrophobic domains, called Ha, Hb, and Hc, located near the C terminus of PopF1, PopF2, and $PopF_{UW551}$, were predicted to form putative membrane-spanning segments (Fig. 4). The TMpred scores for Ha (PopF1 score, 818; PopF2 score, 776; $PopF_{UW551}$ score, 811), Hb (PopF1 score, 827; PopF2 score, 827; $PopF_{UW551}$ score, 850), and Hc (PopF1 score, 641; PopF2 score, 641; $PopF_{UW551}$ score, 639) domains in PopF1, PopF2, and $PopF_{UW551}$ were lower than those obtained for $HrpF_{Xcv}$ and $NopX_{NGR}$ H1 and H2 domains. Multiple alignments between PopF1, PopF2, $PopF_{UW551}$, $HrpF_{Xcv}$, and $NopX_{NGR}$ using the Multalin program suggested that the Ha TM domain of PopF proteins might correspond to the H1 domain of $HrpF_{Xcv}$ and $NopX_{NGR}$, whereas the Hc domain might correspond to H2 domains (data not shown). Moreover, the Ha, Hb, and Hc putative TM domains are located in the region of PopF1 and PopF2 which displays similarity to the YopB family. Interestingly, the conserved region in YopB family members contains the two TM domains that have been characterized in these proteins (11) (Fig. 5). The Hc domain of PopF1/PopF2 overlaps the second TM of YopB family proteins, whereas the Ha domain only partially overlaps the first TM of YopB (Fig. 5).

PopF1 and PopF2 both control the interactions with plants. We constructed *popF1* and *popF2* single mutants and *popF1 popF2* double mutants (Fig. 3; see Material and Methods). When inoculated on tomato plants, the *popF1* mutant and the *popF1 popF2* double mutants were unable to cause any wilting symptoms, thus behaving like *hrp* mutants (Fig. 6). In contrast, *popF2* mutants were not affected in pathogenicity compared to the wild-type strain (Fig. 6). This was also true when a lower bacterial inoculum concentration was used (Fig. 6B).

Following infiltration into tobacco leaves, *popF2* mutants did not show any alteration in the HR-inducing ability, but the *popF1* mutant induced a partial and delayed HR. The *popF1 popF2* double mutants did not induce any symptoms on tobacco leaves (Fig. 6C).

To confirm these results, we conducted complementation experiments. *popF1* and *popF2* were cloned into pLAFR6, generating pPopF1 and pPopF2 plasmids (Fig. 3B). These plasmids were introduced in *trans* into *popF1* mutant (GMI1663), *popF2* mutants (GMI1664 and GMI1665), and *popF1 popF2* double mutants (GMI1666 and GMI1667). Interestingly, both pPopF1 and pPopF2 plasmids complemented the *popF1* and *popF1 popF2* mutants for HR induction (Fig. 6C). Disease complementation tests were not carried out, since previous experiments have shown that these kinds of tests only give partial phenotypes due to plasmid loss (50).

We also tested whether the HrpF protein of *Xanthomonas campestris* pv. *campestris*, hereafter called $HrpF_{Xcc}$, could complement the null HR phenotype of *popF1 popF2* mutants. We chose $HrpF_{Xcc}$ because previous experiments showed *trans*-complementation between *X. campestris* pv. *campestris* and GMI1000 *hrp* gene clusters (3). $pHrpF_{Xcc}$, a pLAFR6 derivative carrying $hrpF_{Xcc}$, was introduced into *popF1 popF2* double mutants (strain GMI1666 or GMI1667). Interestingly, we observed a leaky but reproducible HR when strain GMI1666($pHrpF_{Xcc}$) or GMI1667($pHrpF_{Xcc}$) was infiltrated into tobacco leaves at 3×10^7 cells/ml, whereas strains GMI1666 and GMI1667 did not induce any HR at this inoculum concentration (Fig. 6D). No HR was ever observed when $pHrpF_{Xcc}$ was introduced in *trans* into *hrc* mutant strains (data not shown).

Altogether, these results show that the *popF1 popF2* double mutants behave like *hrp* mutants and that the functions of PopF1 and PopF2 are partially redundant and very similar to that of HrpF. However, the relative phenotypes of the *popF1* and *popF2* mutants on tomato and tobacco suggest that *popF1* plays a more important role than *popF2*.

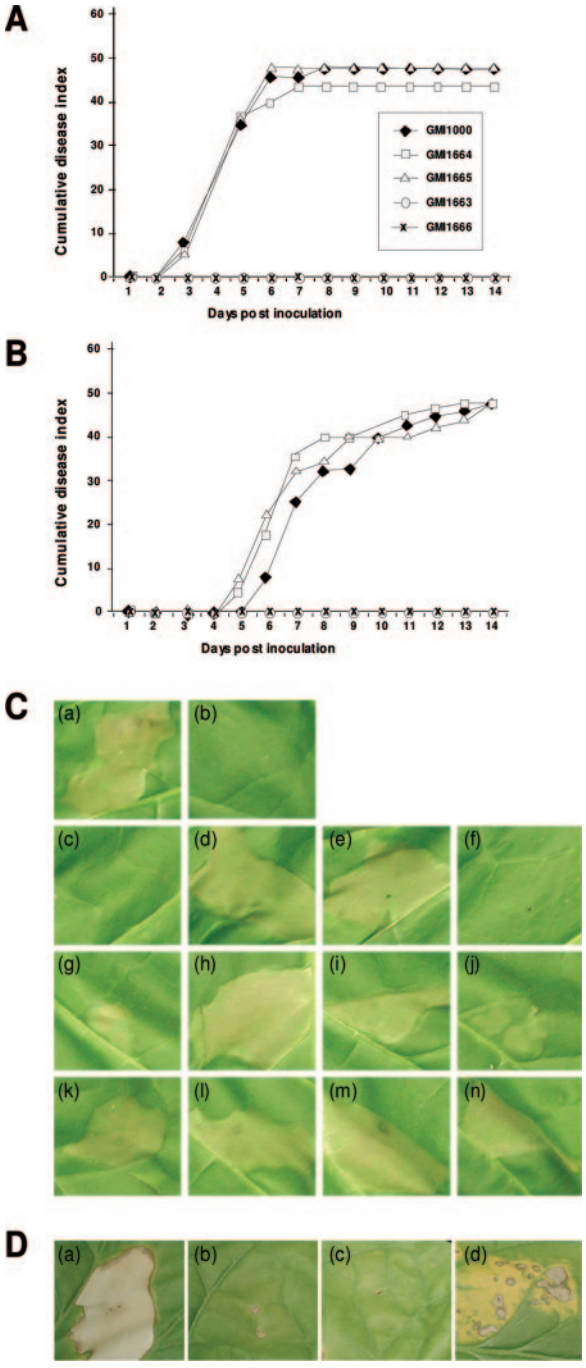

FIG. 6. Pathogenicity, HR, and complementation tests. (A and B) Average disease indices following root inoculation of 12 tomato plants per treatment by bacterial suspensions containing 3×10^8 CFU ml^{-1} (A) or 3×10^7 CFU ml^{-1} (B) of the wild-type strain GMI1000, *popF1* mutant GMI1663, *popF2* mutants GMI1664 and GMI1665, and *popF1 popF2* double mutant GMI1666. These assays were repeated at least three times for each strain. Mutant GMI1667 (*popF1 popF2*) was also tested and gave results similar to those for mutant GMI1666, but it was not shown for clarity of the figure. (C) HR tests and complementation experiments with pPopF1 and pPopF2. Tobacco (cultivar Bottom Special) leaf shows responses 24 h after infiltration by bacterial suspensions (3×10^7 CFU ml^{-1}) of *R. solanacearum*: (a) wild-type strain GMI1000, (b) *hrcS* mutant GMI1402, (c) *popF1 popF2* mutant GMI1666, (d) GMI1666 carrying pPopF1 plasmid (GMI1666/pPopF1), (e) GMI1666/pPopF2, (f) GMI1666/pLAFR6, (g) *popF1* mutant GMI1663, (h) GMI1663/pPopF1, (i) GMI1663/pPopF2, (j) GMI1663/pLAFR6, (k) *popF2* mutant GMI1665, (l) GMI1665/pPopF1, (m) GMI1665/pPopF2, and (n) GMI1665/pLAFR6. (D) Complementation experiments with $pHrpF_{Xcc}$. Tobacco (cultivar Bottom Special) leaf shows responses 36 h after infiltration by suspensions (3×10^7 CFU ml^{-1}) of *R. solanacearum* wild-type strain GMI1000 (a), *hrpB* mutant GMI1525 (b), *popF1 popF2* double mutant GMI1666 (c), and mutant GMI1666 carrying $pHrpF_{Xcc}$ plasmid (d).

TABLE 2. β-Galactosidase activity (Miller's units) of GMI1000 derivatives carrying pCZ408 or pCL94

Gene and strain	Activity in medium:	
	B	MMG
popF1		
GMI1000(pCZ408)	6 ± 1	54.6 ± 4.0
GMI1525*hrpB*(pCZ408)	3.3 ± 1.5	2.3 ± 0.6
popF2		
GMI1000(pCL94)	18.3 ± 1.5	20.3 ± 1.2
GMI1525*hrpB*(pCL94)	19 ± 1.0	8.7 ± 0.6

Values are the averages of at least three independent experiments.

Do *popF1* and *popF2* belong to the hrpB regulon? On the megaplasmid, both *popF1* and *popF2* ORFs are preceded by ORFs having a reverse orientation compared to their own orientation. Moreover, *popF1* and *popF2* coding sequences are followed by clear Rho-independent transcription termination sequences (Fig. 3). Altogether, these data and complementation results suggest that *popF1* and *popF2* are monocistronic operons transcribed from their own promoters.

The start codon of PopF1 is preceded by 313 nucleotides of noncoding DNA, whereas a 264-nucleotide noncoding DNA region precedes the PopF2 ORF. The sequence spanning −130 to 0 nucleotides upstream of both ORFs shares very significant homology (82% identity), whereas DNA regions further upstream are not similar. Interestingly, the promoter region of $popF_{UW551}$ is highly similar to those of *popF1* and *popF2*, whereas that of $popX_{UW551}$ does not show significant similarities (Fig. 2B).

A conserved DNA motif, called the hrp_{II} box, required for the regulation of *hrp* genes by the HrpB regulatory protein (20), was detected in the conserved upstream regions of *popF1* and *popF2* three nucleotides downstream of the beginning of the homologous region (Fig. 2B). The hrp_{II} boxes of *popF1* and *popF2* are located 101 bp and 98 bp upstream of their respective initiation codons, suggesting that *popF1* and *popF2* belong to the *hrpB* regulon.

In order to study the regulation of these genes, DNA fragments located upstream of *popF1* (600 bp) and *popF2* (771 bp) start codons were cloned upstream of a promoterless *lacZ* gene in a reporter plasmid, giving pCZ408 and pCL94, respectively. These constructs were introduced into the wild-type strain or into the *hrpB* mutant GMI1525, and the production of β-galactosidase activity was measured after growth in rich medium (B) or minimal medium (MMG).

popF1 is not expressed in rich medium and is activated in minimal medium in an *hrpB*-dependent manner (Table 2). However, *popF2* showed a similar and low level of transcription in both rich and minimal media, which was reduced by a

twofold factor in the *hrpB* background in minimal medium but was unchanged in B medium. In addition, recently, a transcriptome analysis conducted in minimal medium clearly established that *popF1* and *popF2* are both positively regulated by *hrpB* (55). Clearly, *popF1* belongs to the *hrpB* regulon, but the regulation of *popF2* may be more complex, as our results obtained in minimal medium suggest that this gene is only partially regulated by *hrpB* (Table 2).

PopF1 and PopF2 are Hrp secreted but are not required for Pop secretion. Comparison by SDS-PAGE analysis of CSP-CRs of the wild-type strain with *popF1*, *popF2*, or *popF1 popF2* mutants carrying pAM5 indicated that the 80-kDa band might correspond to PopF1, since this band disappeared in CSP-CRs of the *popF1* or *popF1 popF2* mutants but not from those of the *popF2* mutants (Fig. 1B), thus confirming our previous observations based on N-terminal sequence comparisons.

Furthermore, the analysis of CSP-CRs of these mutants showed that the secretion of PopA and PopB, two effector proteins of strain GMI1000, was not impaired, thus showing that *popF1* and *popF2* are not required for the secretory process in vitro (Fig. 1B). This observation was confirmed by Western analysis using an anti-PopA polyclonal antibody (data not shown).

In order to study PopF2 secretion, we introduced an immunological His_6 tag at the C-terminal end of PopF2. The PopF2-His_6 gene construct was marker exchanged into strain GMI1000 and in the two mutants GMI1402 (*hrcS*) and GMI1410 (*hrpY*), generating strains in which the *popF2* gene was replaced by the His_6-tagged derivative (see Materials and Methods). These strains were grown in MMG supplemented with Congo red, and the presence of PopF2-His_6 was analyzed by Western blotting using an anti-His_6 monoclonal antibody. A signal, corresponding in size (~83 kDa) to *popF2*-His_6, was detected in the CSP-CR from the wild-type derivative but not from the *hrp* mutant derivatives (Fig. 1D). This band was never detected in the CSP-CR of GMI1000, GMI1631 (*popB*-His_6), or GMI1626 (*popC*-His_6), showing that this signal seems specific for the PopF2-His_6 fusion protein. We also noticed that this band was not detectable in the cell lysates prepared from the wild-type derivative or the *hrp* mutants carrying the *popF*2-His_6 construct. This differs from previous observations of Pop proteins, which were always detected in the lysates of the wild type and of the *hrp* mutants (28, 46).

PopF1 and PopF2 are required for the translocation of AvrA. Since PopF1 and PopF2 seem to belong to the HrpF family of translocators, we tested whether these proteins control the translocation of the avirulence protein AvrA. The *avrA* gene was characterized from *R. solanacearum* strain AW1 and was supposed to control HR development on tobacco plants, possibly at the species level (13). The strain GMI1000 possesses an *avrA* homologue named $avrA_{GMI1000}$. This gene, previously referred to as RSc0608/brg46, is *hrpB* regulated, as shown in a study of strain GMI1000 TTSS candidate effectors (21). A GMI1000 *avrA* mutant is unable to induce the HR on *Nicotiana benthamiana* leaves (19). Transient expression of $avrA_{GMI1000}$ in *N. benthamiana* cells results in HR induction, suggesting that this protein acts inside plant cells. Furthermore, experiments using the CyaA translocation reporter system in our laboratory have shown that this protein, and several other TTSS candidate effectors of strain GMI1000, are translocated into plant cells (19, 21). Translocation is tested by fusing the coding sequence of a candidate type III translocated protein to *cyaA*, the calmodulin-dependent adenylate cyclase domain of *Bordetella pertussis* cyclolysin (14, 66, 67). Since cAMP production by CyaA is dependent on calmodulin, which is only present in eukaryotic cells, the production of cAMP indicates that the CyaA domain was translocated into eukaryotic cells.

The plasmid pSC163 containing the translational fusion $AvrA_{1-99}$::CyaA′ was introduced into strains GMI1000, GMI1402 (*hrcS*), GMI1663 (*popF1*), GMI1664 (*popF2*), and GMI1666 (*popF1 popF2*). The strains were grown in MMG supplemented with Congo red, and the CSP-CR and CLP-CR were analyzed by Western blotting with anti-CyaA antibodies. The fusion protein was found to be stable in the different strains (Fig. 7), and it was secreted in the extracellular medium in an Hrp-dependent manner (Fig. 7A). The $AvrA_{1-99}$::CyaA′ construct was still secreted in *popF1*, *popF2*, and *popF1 popF2* mutants.

To study translocation, each strain was infiltrated into *Nicotiana benthamiana* leaves. Plant cell extracts were prepared 7 h later and assayed for cAMP. When expressed in the wild-type strain, the $AvrA_{1-99}$::CyaA′ fusion protein resulted in higher cAMP levels than in the controls. The cAMP levels produced by the *hrp* mutant and the *popF1 popF*2 double mutant producing $AvrA_{1-99}$::CyaA′ were very low and comparable to those of negative controls (Fig. 7). cAMP levels found using the *popF1* mutant were low but significantly higher than those of *hrp* mutants and controls. *popF2* mutants produced slightly lower levels than those obtained with the wild-type strain. The levels of cAMP produced by the mutants reflected the intensity of the HR they induced on tobacco leaves (Fig. 6B). We conclude that AvrA is translocated into plant cells and that full translocation activity requires both a functional type III secretion machinery and the presence of PopF1 and PopF2.

Is PopF1 associated with Hrp pili? SDS-PAGE analysis of GMI1000 Hrp pili preparations showed that the *hrpY* gene encodes an abundantly present 7-kDa protein (75). A closer analysis revealed the presence of a double band in the upper part of the gel corresponding to proteins with an apparent mass of 80 kDa. Interestingly, the more diffuse upper band of this doublet seems to disappear in preparations of *hrp* mutants, whereas the lower band does not. In order to test whether this upper 80-kDa protein could correspond to PopF1 or PopF2, we compared pili preparations of the wild-type strain with those of *popF1* or *popF2* mutants by SDS-PAGE and Coomassie blue staining (Fig. 1C). The double band was clearly visible in preparations of strain GMI1000. The upper band disappeared in preparations of *hrcV* and *popF1* mutants but was still present in preparations of *popF2* mutants. The 7-kDa HrpY protein which is absent in the *hrcV* preparation was still visible in preparations of *popF1*, *popF2*, and *popF1 popF2* mutants. Electron microscopic examinations of negatively stained *popF1*, *popF2*, and *popF1 popF2* mutants showed that the production of Hrp pili was not impaired in these mutants (data not shown).

These results suggest that PopF1 protein might be associated with the Hrp pilus. They also indicate that PopF1 and PopF2 are not required for its assembly.

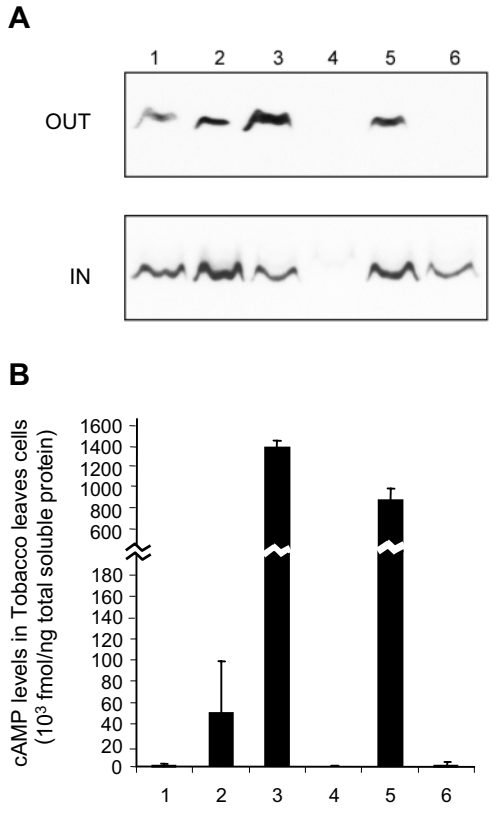

FIG. 7. Translocation of AvrA::CyaA′ fusion proteins into plant cells through the TTSS. (A) Immunoblot analysis of $AvrA_{1-99}$::CyaA′ protein fusions in supernatants and cellular lysates. Bacterial strains were cultivated in MMG supplemented with Congo red. Concentrated supernatant preparations (CSP-CR) (OUT) and concentrated lysate preparations (CLP-CR) (IN) were prepared from these cultures, and their protein contents were separated by SDS-PAGE and visualized by immunoblotting with a monoclonal antiserum raised against adenylate cyclase for the following strains: (lane 1) GMI1666 *popF1 popF2* carrying pSC163 (pLAFR6::$AvrA_{1-99}$::CyaA′), (lane 2) GMI1663*popF1*/pSC163, (lane 3) GMI1000/pSC163, (lane 4) GMI1000, (lane 5) GMI1664*popF2*/pSC163, and (lane 6) GMI1402*hrcS*/pSC163. Control experiments with an anti-LacI antibody that detected the intracellular LacI protein demonstrated that cell lysis could not account for the signals detected with anti-CyaA′ antibody (data not shown). (B) Cya translocation assays showing adenylate cyclase activity of the $AvrA_{1-99}$::CyaA′ fusion protein. Measurements of cAMP detected in bottom special tobacco leaf cells 7 h postinoculation with derivatives of the wild-type strain GMI1000 and *hrp* and *popF* mutants. For a particular strain, the means and standard deviations were calculated from measurements of three independent samples. Bacterial strains were the following: (lane 1) GMI1666 carrying pSC163 (pLAFR6::$AvrA_{1-99}$::CyaA′), (lane 2) GMI1663*popF1*/pSC163, (lane 3) GMI1000/pSC163, (lane 4) GMI1000, (lane 5) GMI1664*popF2*/pSC163, and (lane 6) GMI1402*hrcS*/pSC163.

PopF, HrpF, and NopX proteins can be classified into three distinct groups. The existence of four putative translocators in *R. solanacearum* prompted us to analyze the relationships between these proteins and HrpF or NopX protein. The comparison of whole-protein aa sequences, using alignments generated by ClustalW (72), showed that these proteins are well conserved. In addition, they can be subdivided into three major groups corresponding to their taxonomic origin: the NopX and HrpF proteins form two distinct groups, whereas PopF1, PopF2, and $PopF_{UW551}$ are associated in a third group, indicating that these three latter proteins are more closely related to one another (Fig. S1 in the supplemental material). Interestingly, $PopX_{UW551}$ is not in the PopF group but is positioned between PopF and NopX groups, apparently more closely related to the NopX group. Furthermore, this analysis places the PopF group closer to NopX proteins than to HrpF proteins.

Differential evolution of PopF, HrpF, and NopX domains. A closer analysis reveals that the degree of similarity between PopF, PopX, HrpF, and NopX proteins varies greatly in different parts of these proteins. Multiple alignment and similarity comparisons provide strong evidence that PopF, PopX, NopX, and HrpF proteins can in fact be subdivided into the following four domains: an N-terminal domain (Nt), a repeat domain (R), a median domain (M), and a C-terminal domain (Ct) (Fig. 4). Interestingly, ClustalW analysis (Fig. S1 in the supplemental material) reveals that the grouping for each of these domains does not always match that for the entire protein, thus suggesting a certain independence in the evolution of the various domains and probably reflecting their different functions.

The R domain corresponds to repeated sequences, named R1 and R2, found in $HrpF_{Xcv}$ (34) (Fig. 4). The analysis of PopF1, PopF2, and $PopF_{UW551}$ revealed two 90- to 95-aa direct imperfect repeats in the N-terminal regions that partially match the R1 and R2 repeats of $HrpF_{Xcv}$. The three NopX proteins and $PopX_{UW551}$ have only one copy of this region, whereas all HrpF proteins have two copies of the direct repeat, with the exception of $HrpF_{Xcc}$, which contains a third copy, named R3 (Fig. 4). The R domains of NopX, HrpF, and PopF proteins form three separate groups which are in line with the taxonomic classification (Fig. S1C in the supplemental material). The particularly large branch lengths of the R1 repeats of PopF2 and $PopF_{UW551}$ suggest that the evolution of these repeats is relatively rapid (Fig. S1E in the supplemental material). Furthermore, the R1 and R2 repeats of PopF2 appear more divergent than those of PopF1.

The Nt domain is the most divergent in all groups (Fig. S1C in the supplemental material), suggesting that this domain is also subject to rapid evolution. The Nt domain of $PopF_{UW551}$ appears more closely related to the PopF2 Nt domain than to the PopF1 Nt domain, in contrast to the M, Ct, and R domains of these proteins. Furthermore, it is worth noting a closer relationship between the Nt domain of $PopX_{UW551}$ and the PopF Nt domains compared to the NopX Nt domain, whereas the other domains of this protein are more closely related to NopX proteins. Therefore, it is possible that the evolution of this domain is influenced by factors specific to each bacterial species. Taken together, these comparative analyses will certainly be very useful in future structure/function studies and in understanding the evolution of translocons in phytopathogenic bacteria.

DISCUSSION

In this study, we characterized two novel proteins, PopF1 and PopF2, secreted through the TTSS of *R. solanacearum* strain GMI1000. These two proteins are homologous to one another, and they share high similarities to NopX proteins from nitrogen-fixing symbiotic rhizobia and to HrpF proteins

from *Xanthomonas* species. *popF1* and *popF*2 do not seem to have the same importance in interactions with plants in our experimental system. *popF1* plays a crucial role for disease development on tomato plants, whereas *popF2* is not required for pathogenicity on this plant. The situation was slightly different for HR elicitation on tobacco leaves. The *popF*2 mutants gave HR very similar to those induced by the wild-type strain, whereas the *popF1* mutant elicited a leaky and delayed HR. The *popF1 popF2* double mutants did not induce any HR symptoms. This suggests that although *popF1* seems to play a major part in HR induction, *popF*2 also seems to contribute to the development of this defense reaction. This hypothesis was confirmed by complementation experiments showing that when provided in *trans*, *popF1* or *popF2* can restore the ability to induce a normal HR to *popF1 popF2* double mutants. The number of copies of pLAFR6 derivatives carrying *popF1* or *popF2* in these experiments might explain the appearance of normal rather than leaky HR. Are the differences observed between tomato and tobacco tests, concerning *popF1* and *popF2*, due to plant or tissue specificities or to the type of symptoms that are studied (disease versus HR)? It will be interesting to extend our analysis to a broader range of plants to try to answer to these questions.

Our data strongly suggest that both PopF1 and PopF2 act as translocators for the *R. solanacearum* TTSS. These two proteins share characteristics specific to TTSS translocators: *popF1 popF2* double mutants display an Hrp^- phenotype on plants, but they retain the ability to secrete Pop and $AvrA_{1\text{-}99}$::CyaA′ proteins in culture via the TTSS. However, both PopF1 and PopF2 are required for efficient translocation of $AvrA_{1\text{-}99}$::CyaA′ protein into tobacco cells. This assay reflects the in planta response, since we observed a good correlation between the translocation efficiency of $AvrA_{1\text{-}99}$::CyaA′ and the HR phenotype of *popF1*, *popF2*, and *popF1 popF2* mutants. Finally, a *popF1 popF2* mutant was partially complemented by the HrpF translocator of *X. campestris* pv. *campestris*, thus showing the functional similarity of *R. solanacearum* and *Xanthomonas* putative translocators.

In xanthomonads, the *hrpF* gene is unique and located very close to the *hrp* cluster in a region showing a high degree of variability, called the HrpF Peninsula (41, 47, 68). In *S. fredii* NGR234 and *M. loti*, *nopX* exists as a single copy and is located inside the TTSS gene cluster carried by symbiotic islands or plasmids (23, 38, 44). The situation seems slightly different in *R. solanacearum*, since we identified two genes coding for putative translocators. In strain GMI1000, these genes are not located in close vicinity of the *hrp* gene cluster. The *popF2* gene is located 34 kb to the righthand end of the *hrp* gene cluster, and *popF1* maps 817 kb further on. This region harbors at least 40 complete or truncated insertion elements, several transposase or integrase genes, and 12 DNA regions classified as ACURs (alternative codon usage regions), which may have been acquired through horizontal transfer (46, 64). In *R. solanacearum*, the *hrp* locus and its flanking regions cannot be considered a pathogenicity island, but it has most likely coevolved with the genome (64). Therefore, it is possible that the presence of *popF1* and *popF2* reflects the long evolution of this region, which has been submitted to several rearrangements. Is the presence of *popF1* and *popF2* the result of a duplication of an ancestral gene? Interestingly, strain UW551 also possesses two genes, $popF_{UW551}$ and $popX_{UW551}$, which code for putative related translocators. However, although $PopF_{UW551}$ is closely related to PopF1 and PopF2, $PopX_{UW551}$ is clearly different and seems to be more related to NopX proteins. Our phylogenetic study showed that NopX, HrpF, and PopF proteins form three distinct branches corresponding to their taxonomic origin, whereas $PopX_{UW551}$ is positioned between PopF and NopX groups, thus forming a distinct and specific branch. No direct ortholog of $PopX_{UW551}$ was found in strain GMI1000. Therefore, this gene seems unique to strain UW551. Interestingly, its location in the UW551 genome corresponds to a gene of GMI1000 which is absent in the UW551 genome (Fig. 3). This suggests that this locus is variable in *R. solanacearum* strains. It also raises the question of the origin of this gene. Concerning $popF_{UW551}$, although it displays the best homologies with *popF2*, its location in the UW551 genome suggests that it corresponds to *popF1* of GMI1000. This observation, and the fact that the DNA region carrying *popF2* is not present in strain UW551, strongly favors the duplication hypothesis. Moreover, the importance of *popF1* in the interaction with plants could suggest that this gene corresponds to the ancestral gene. However, we cannot rule out that the evolution of this gene after the putative duplication event has contributed to this gain of function. Alternatively, the fact that PopF2 and $PopF_{UW551}$ seem to be more related to one another could suggest that they correspond to the ancestral gene. In GMI1000, it seems that the evolution of *popF2* is accelerated compared to that of *popF1*. Thus, the presence of $popX_{UW551}$ may also have influenced the evolution of $popF_{UW551}$. This raises the following question: does the presence of two translocator genes in one genome influence their evolution? It will now be interesting to see whether $popF_{UW551}$ and $popX_{UW551}$ are both functional and serve as translocators for the TTSS and if they play similar roles in pathogenicity. It is worth noting that both genes possess an hrp_{II} box in their promoter region (see reference 25 and Fig. 2), suggesting that they belong to the HrpB regulon and thus that they are related to the TTSS. Why do the two *R. solanacearum* strains studied so far carry two putative TTSS translocators, and why are these translocators different? Are there any relationships with their host range, their pathogenicity, or their phylogeny? *R. solanacearum* strains are classified into four phylotypes which seem to have evolved separately due to geographical isolation (25). Strain GMI1000 belongs to phylotype I, whereas UW551 is a member of phylotype II. In general, strains of phylotype I are thought to have a broader host range than strains of phylotype II, although this has recently been questioned (25). It will now be interesting to compare several *R. solanacearum* strains of different origins and phylotypes to see whether the presence of two sets of translocators is the rule or the exception in *R. solanacerum* strains and whether this is related to their phylogeny.

As mentioned above, the two translocators of strain GMI1000 do not seem to have the same importance for pathogenicity. Several explanations can be put forward to explain the differential behavior of these two genes. The first one is related to differences in expression of these genes. The expression of *popF1* follows a typical *hrp* pattern; this gene is not expressed in rich medium and is induced in minimal medium in an *hrpB*-dependent manner. In contrast, by using transcriptional fusion with promoter of *popF2*, the level of transcription of this gene

appeared similar in rich and minimal media and lower than that observed for *popF1* in minimal medium. Our data and transcriptome analyses (55) also showed that *popF2* is only partially regulated by HrpB in minimal medium. Did we introduce a bias when studying the expression of genes by cloning their promoter into reporter plasmids? Further experiments are needed to answer this question. The promoter regions of *popF1* and *popF2* share high similarity with one another, and they both contain an hrp_{II} box, the presumed HrpB binding site. However, the hrp_{II} boxes of these two genes differ by one nucleotide, and there are other differences in the promoter regions. A comparative analysis of these two promoters might help to characterize the molecular basis explaining their differential behavior in HrpB regulation.

A difference in expression is not the only possibility that can be put forward to explain the differences between *popF1* and *popF2* mutants. PopF1 and PopF2 proteins are very similar, but they display differences that might explain their differential behavior. Proteins in this translocator family can be subdivided into four domains, called Nt, R, M, and Ct, showing different levels of conservation. Each of these domains might correspond to different functions that are not subjected to the same selective pressure. The N termini of PopF1, PopF2, and $PopF_{UW551}$, encompassing Nt and R1 domains, appears to be less conserved than the C termini (R2, M, and Ct domains), affecting the pIs of these proteins (pIs of PopF1, PopF2, and $PopF_{UW551}$ are 5.82, 7.14, and 5.73, respectively). The pIs of PopF1 and $PopF_{UW551}$ mostly correspond to the pI of HrpF/NopX family members, which ranges from 5.20 to 5.52, the only exception being $HrpF_{Xcc}$, with a pI of 6.01. Therefore, it seems that PopF2 occupies a particular place in this family. Do the differences observed between PopF1 and PopF2 N-terminal regions have an effect on the functionality or stability of PopF2, thus explaining its minor role in the interaction with plants? The Nt domain might be required for TTSS secretion by analogy to $HrpF_{Xcv}$, since a type III secretion signal was identified in the N terminus of this protein (12). The R domain is composed of two imperfect repeats (R1 and R2) in PopF1, PopF2, and $PopF_{UW551}$ and in most HrpF proteins, whereas this region is not duplicated in NopX or $PopX_{UW551}$ proteins. We observed that $HrpF_{Xcc}$ carries three repeats, suggesting a high variability of this region. Is there any biological significance for the presence of these repeats and their number? It is worth noting that removal of R1 repeat in $HrpF_{Xcv}$ does not affect its function (34).

The M domain is the most conserved domain among proteins of the HrpF/NopX/PopX/PopF family. The TM regions present in the C-terminal part of this domain might be related to the putative function of these proteins. The number of these domains varies from one in $PopX_{UW551}$ and $NopX_{Ml}$ of *M. loti* to two in other NopX proteins and in HrpF members and to three in PopF1, PopF2, and $PopF_{UW551}$. In *Xanthomonas campestris* pv. *vesicatoria*, Büttner and colleagues (12) showed that the TM domains are essential for HrpF function. $HrpF_{Xcv}$ has a lipid binding activity and induces pore formation in lipid bilayers (12). However, TM regions were not required for the lipid binding activity, suggesting that HrpF interacts with lipids via nonhydrophobic regions. TM domains have also been detected in translocators of animal pathogens such as IpaB, YopB, SipB, and EpsD of type III translocons of *Shigella*, *Yersinia*, *Salmonella*, and *E. coli*, respectively (see reference 11 for a review). Interestingly, the region of PopF and HrpF proteins carrying the putative TM domains shares a weak but significant similarity with a central region highly conserved in proteins belonging to the YopB translocator family. In YopB family members this region contains two TM domains (11). Multiple sequence alignments indicated that the TM domains of PopF and YopB proteins partially overlap. Although the occurrence of structural homologies between HrpF and YopB has already been mentioned (11, 31), this work is the first showing the existence of similarities between TTSS translocators of animal and plant pathogens. YopB can integrate into synthetic membranes, where it is associated with channel formation (70). However, this protein does not act alone to translocate effectors inside animal cells but does so in association with YopD and LcrV (33). Considering additionally the analogy to animal pathogen translocons, PopF1 and PopF2 are most likely type III translocators, and the possible involvement of accessory proteins should now be investigated. In *P. syringae*, proteins displaying high similarities with HrpF, NopX, or PopF1/PopF2 were not reported (10), but two candidate translocators, HrpK and HrpZ, have been identified. HrpK possesses all the characteristics of translocators: it has a TM domain and displays a very weak similarity to PopF, HrpF, and NopX. It is required for the translocation of Avr proteins (56). However, an *hrpK* mutation was not complemented by the *hrpF* gene of *X. campestris* pv. *vesicatoria* provided in *trans*. HrpZ, the other putative translocator of *P. syringae*, is a harpin which is capable of forming pores in lipid bilayers (48). Whether HrpK and HrpZ interact with one another to form a translocon has not yet been tested. Harpin-like proteins have been characterized in *R. solanacearum* and *Xanthomonas* sp. (5, 41, 78). In *X. campestris* pv. *vesicatoria*, XopA, which is secreted by the TTSS and which displays homologies with HpaG and Hpa1 harpin-like proteins of *Xanthomonas axonopodis* pv. *glycines* and *Xanthomonas oryzae* pv. *oryzae* (40, 68), has been suggested to be a component of the type III translocon (54). Indeed, a *xopA* mutant is reduced in pathogenicity without affecting type III secretion in vitro. It will be interesting to test whether the *R. solanacearum* PopA harpin-like elicitor is a putative translocator and interacts with PopF1 or PopF2.

Another question concerns whether the PopF1/PopF2 translocon forms a continuous conduit with the Hrp pilus or whether it functions at a distance to mediate effector delivery. In *Y. pseudoturberculosis*, YopB provided in *trans* cannot promote YopE translocation, thus suggesting that YopB must remain in the vicinity of the needle complex or even that there is continuous contact between YopB and the needle (62). In *X. campestris* pv. *vesicatoria*, immunoelectron microscopy experiments showed that $HrpF_{Xcv}$ is in close contact with the Hrp pilus (76). However, it was not possible to conclude whether this localization was due to the detection of secreted $HrpF_{Xcv}$ through the pilus conduit or whether it reflects an association between the translocon and the pilus. In *S. fredii*, Western blot analysis with antibodies raised against NopX revealed that this protein is associated with the TTSS pili (43). In NGR234, Saad and colleagues (63) showed that the TTSS pili are mainly composed of three proteins: NopA, the major component of the TTSS-pilus, NopB, a protein resembling FlgK, a protein

involved in flagellum assembly, and NopX (63). In *R. solanacearum*, PopF1 is also associated with Hrp pili, as determined by SDS-PAGE analysis of purified pili preparations. Is the association of PopF, HrpF, or NopX with TTSS pili fortuitous, depending on specific properties of these proteins that allow nonspecific attachment to pili? Alternatively, does the presence of these proteins reflect continuity between the pilus and the translocon? Using the two-hybrid system, we were unable to detect an interaction between PopF1 and HrpY, the major component of *R. solanacearum* Hrp pilus. However, we cannot exclude that Hrp pili contain minor components that have not yet been detected and which connect the pilus and the translocon. Further work is needed to answer these questions.

ACKNOWLEDGMENTS

We thank N. Grimsley for critical comments on the manuscript and J. Gouzy and S. Carrere for help in sequence analysis.

M. Guéneron, S. Cunnac, and D. Meyer were supported by grants from the Ministère de la Recherche et de l'Enseignement Supérieur. We gratefully acknowledge financial support from the Département Santé des Plantes et Environnement de L'Institut National de la Recherche Agronomique.

REFERENCES

1. **Alfano, J. R., and A. Collmer.** 1997. The type III (Hrp) secretion pathway of plant pathogenic bacteria: trafficking harpins, Avr proteins, and death. J. Bacteriol. **179:**5655–5662.
2. **Alfano, J. R., and A. Collmer.** 2004. Type III secretion system effector proteins: double agents in bacterial disease and plant defense. Annu. Rev. Phytopathol. **42:**385–414.
3. **Arlat, M., C. L. Gough, C. E. Barber, C. Boucher, and M. J. Daniels.** 1991. *Xanthomonas campestris* contains a cluster of hrp genes related to the larger hrp cluster of *Pseudomonas solanacearum*. Mol. Plant-Microbe Interact. **4:**593–601.
4. **Arlat, M., C. L. Gough, C. Zischek, P. A. Barberis, A. Trigalet, and C. A. Boucher.** 1992. Transcriptional organization and expression of the large hrp gene cluster of *Pseudomonas solanacearum*. Mol. Plant-Microbe Interact. **5:**187–193.
5. **Arlat, M., F. Van Gijsegem, J. C. Huet, J. C. Pernollet, and C. A. Boucher.** 1994. PopA1, a protein which induces a hypersensitivity-like response on specific petunia genotypes, is secreted via the Hrp pathway of *Pseudomonas solanacearum*. EMBO J. **13:**543–553.
6. **Ausubel, F. M., R. Brent, R. E. Kingston, D. D. Moore, J. G. Seidman, J. A. Smith, and K. Struhl.** 1996. Current protocols in molecular biology, Wiley, New York, N.Y.
7. **Bogdanove, A. J., S. V. Beer, U. Bonas, C. A. Boucher, A. Collmer, D. L. Coplin, G. R. Cornelis, H. C. Huang, S. W. Hutcheson, N. J. Panopoulos, and F. Van Gijsegem.** 1996. Unified nomenclature for broadly conserved *hrp* genes of phytopathogenic bacteria. Mol. Microbiol. **20:**681–683.
8. **Boucher, C. A., P. A. Barberis, A. P. Trigalet, and D. A. Demery.** 1985. Transposon mutagenesis of *Pseudomonas solanacearum*: isolation of Tn5-induced avirulent mutants. J. Gen. Microbiol. **131:**2449–2457.
9. **Brau, B., U. Pilz, and W. Piepersberg.** 1984. Genes for gentamicin-(3)-N-acetyltransferases III and IV: I. Nucleotide sequence of the AAC(3)-IV gene and possible involvement of an IS140 element in its expression. Mol. Gen. Genet. **193:**179–187.
10. **Buell, C. R., V. Joardar, M. Lindeberg, J. Selengut, I. T. Paulsen, M. L. Gwinn, R. J. Dodson, R. T. Deboy, A. S. Durkin, J. F. Kolonay, R. Madupu, S. Daugherty, L. Brinkac, M. J. Beanan, D. H. Haft, W. C. Nelson, T. Davidsen, N. Zafar, L. Zhou, J. Liu, Q. Yuan, H. Khouri, N. Fedorova, B. Tran, D. Russell, K. Berry, T. Utterback, S. E. Van Aken, T. V. Feldblyum, M. D'Ascenzo, W. L. Deng, A. R. Ramos, J. R. Alfano, S. Cartinhour, A. K. Chatterjee, T. P. Delaney, S. G. Lazarowitz, G. B. Martin, D. J. Schneider, X. Tang, C. L. Bender, O. White, C. M. Fraser, and A. Collmer.** 2003. The complete genome sequence of the Arabidopsis and tomato pathogen *Pseudomonas syringae pv. tomato* DC3000. Proc. Natl. Acad. Sci. USA **100:**10181–10186.
11. **Buttner, D., and U. Bonas.** 2002. Port of entry–the type III secretion translocon. Trends Microbiol. **10:**186–192.
12. **Buttner, D., D. Nennstiel, B. Klusener, and U. Bonas.** 2002. Functional analysis of HrpF, a putative type III translocon protein from *Xanthomonas campestris* pv. *vesicatoria*. J. Bacteriol. **184:**2389–2398.
13. **Carney, B. F., and T. P. Denny.** 1990. A cloned avirulence gene from *Pseudomonas solanacearum* determines incompatibility on *Nicotiana tabacum* at the host species level. J. Bacteriol. **172:**4836–4843.
14. **Casper-Lindley, C., D. Dahlbeck, E. T. Clark, and B. J. Staskawicz.** 2002. Direct biochemical evidence for type III secretion-dependent translocation of the AvrBs2 effector protein into plant cells. Proc. Natl. Acad. Sci. USA **99:**8336–8341.
15. **Chang, J. H., J. M. Urbach, T. F. Law, L. W. Arnold, A. Hu, S. Gombar, S. R. Grant, F. M. Ausubel, and J. L. Dangl.** 2005. A high-throughput, near-saturating screen for type III effector genes from *Pseudomonas syringae*. Proc. Natl. Acad. Sci. USA **102:**2549–2554.
16. **Cornelis, G. R.** 2002. *Yersinia* type III secretion: send in the effectors. J. Cell Biol. **158:**401–408.
17. **Cornelis, G. R., A. Boland, A. P. Boyd, C. Geuijen, M. Iriarte, C. Neyt, M. P. Sory, and I. Stainier.** 1998. The virulence plasmid of *Yersinia*, an antihost genome. Microbiol. Mol. Biol. Rev. **62:**1315–1352.
18. **Cornelis, G. R., and F. Van Gijsegem.** 2000. Assembly and function of type III secretory systems. Annu. Rev. Microbiol. **54:**735–774.
19. **Cunnac, S.** 2004. Genomewide identification of type III secretion system effectors from the bacterial plant pathogen *Ralstonia solanacearum*. Ph.D. thesis. Paul Sabatier University, Toulouse, France.
20. **Cunnac, S., C. Boucher, and S. Genin.** 2004. Characterization of the *cis*-acting regulatory element controlling HrpB-mediated activation of the type III secretion system and effector genes in *Ralstonia solanacearum*. J. Bacteriol. **186:**2309–2318.
21. **Cunnac, S., A. Occhialini, P. Barberis, C. Boucher, and S. Genin.** 2004. Inventory and functional analysis of the large Hrp regulon in *Ralstonia solanacearum*: identification of novel effector proteins translocated to plant host cells through the type III secretion system. Mol. Microbiol. **53:**115–128.
22. **Da Silva, A. C., J. A. Ferro, F. C. Reinach, C. S. Farah, L. R. Furlan, R. B. Quaggio, C. B. Monteiro-Vitorello, M. A. Van Sluys, N. F. Almeida, L. M. Alves, A. M. do Amaral, M. C. Bertolini, L. E. Camargo, G. Camarotte, F. Cannavan, J. Cardozo, F. Chambergo, L. P. Ciapina, R. M. Cicarelli, L. L. Coutinho, J. R. Cursino-Santos, H. El-Dorry, J. B. Faria, A. J. Ferreira, R. C. Ferreira, M. I. Ferro, E. F. Formighieri, M. C. Franco, C. C. Greggio, A. Gruber, A. M. Katsuyama, L. T. Kishi, R. P. Leite, E. G. Lemos, M. V. Lemos, E. C. Locali, M. A. Machado, A. M. Madeira, N. M. Martinez-Rossi, E. C. Martins, J. Meidanis, C. F. Menck, C. Y. Miyaki, D. H. Moon, L. M. Moreira, M. T. Novo, V. K. Okura, M. C. Oliveira, V. R. Oliveira, H. A. Pereira, A. Rossi, J. A. Sena, C. Silva, R. F. de Souza, L. A. Spinola, M. A. Takita, R. E. Tamura, E. C. Teixeira, R. I. Tezza, M. Trindade dos Santos, D. Truffi, S. M. Tsai, F. F. White, J. C. Setubal, and J. P. Kitajima.** 2002. Comparison of the genomes of two *Xanthomonas* pathogens with differing host specificities. Nature **417:**459–463.
23. **Freiberg, C., R. Fellay, A. Bairoch, W. J. Broughton, A. Rosenthal, and X. Perret.** 1997. Molecular basis of symbiosis between *Rhizobium* and legumes. Nature **387:**394–401.
24. **Frithz-Lindsten, E., A. Holmstrom, L. Jacobsson, M. Soltani, J. Olsson, R. Rosqvist, and A. Forsberg.** 1998. Functional conservation of the effector protein translocators PopB/YopB and PopD/YopD of *Pseudomonas aeruginosa* and *Yersinia pseudotuberculosis*. Mol. Microbiol. **29:**1155–1165.
25. **Gabriel, D. W., C. Allen, M. Schell, T. P. Denny, J. T. Greenberg, Y. P. Duan, Z. Flores-Cruz, Q. Huang, J. M. Clifford, G. Presting, E. T. Gonzalez, J. Reddy, J. Elphinstone, J. Swanson, J. Yao, V. Mulholland, L. Liu, W. Farmerie, M. Patnaikuni, B. Balogh, D. Norman, A. Alvarez, J. A. Castillo, J. Jones, G. Saddler, T. Walunas, A. Zhukov, and N. Mikhailova.** 2006. Identification of open reading frames unique to a select agent: *Ralstonia solanacearum* race 3 biovar 2. Mol. Plant-Microbe Interact. **19:**69–79.
26. **Genin, S., and C. Boucher.** 2004. Lessons learned from the genome analysis of *Ralstonia solanacearum*. Annu. Rev. Phytopathol. **42:**107–134.
27. **Gophna, U., E. Z. Ron, and D. Graur.** 2003. Bacterial type III secretion systems are ancient and evolved by multiple horizontal-transfer events. Gene **312:**151–163.
28. **Gueneron, M., A. C. Timmers, C. Boucher, and M. Arlat.** 2000. Two novel proteins, PopB, which has functional nuclear localization signals, and PopC, which has a large leucine-rich repeat domain, are secreted through the hrp-secretion apparatus of *Ralstonia solanacearum*. Mol. Microbiol. **36:**261–277.
29. **Hakansson, S., K. Schesser, C. Persson, E. E. Galyov, R. Rosqvist, F. Homble, and H. Wolf-Watz.** 1996. The YopB protein of *Yersinia pseudotuberculosis* is essential for the translocation of Yop effector proteins across the target cell plasma membrane and displays a contact-dependent membrane disrupting activity. EMBO J. **15:**5812–5823.
30. **Hayward, A. C.** 1991. Biology and epidemiology of bacterial wilt caused by *Pseudomonas Solanacearum*. Annu. Rev. Phytopathol. **29:**65–87.
31. **He, S. Y., K. Nomura, and T. S. Whittam.** 2004. Type III protein secretion mechanism in mammalian and plant pathogens. Biochim. Biophys. Acta **1694:**181–206.
32. **Henke, J. M., and B. L. Bassler.** 2004. Quorum sensing regulates type III secretion in *Vibrio harveyi* and *Vibrio parahaemolyticus*. J. Bacteriol. **186:**3794–3805.
33. **Holmstrom, A., J. Olsson, P. Cherepanov, E. Maier, R. Nordfelth, J. Pettersson, R. Benz, H. Wolf-Watz, and A. Forsberg.** 2001. LcrV is a channel size-determining component of the Yop effector translocon of *Yersinia*. Mol. Microbiol. **39:**620–632.

34. **Huguet, E., and U. Bonas.** 1997. hrpf of *Xanthomonas campestris pv. vesicatoria* encodes an 87-kDa protein with homology to NoIX of *Rhizobium fredii*. Mol. Plant-Microbe Interact. **10:**488–498.
35. **Huynh, T. V., D. Dahlbeck, and B. J. Staskawicz.** 1989. Bacterial blight of soybean: regulation of a pathogen gene determining host cultivar specificity. Science **245:**1374–1377.
36. **Jin, Q., and S. Y. He.** 2001. Role of the Hrp pilus in type III protein secretion in *Pseudomonas syringae*. Science **294:**2556–2558.
37. **Jin, Q., W. Hu, I. Brown, G. McGhee, P. Hart, A. L. Jones, and S. Y. He.** 2001. Visualization of secreted Hrp and Avr proteins along the Hrp pilus during type III secretion in *Erwinia amylovora* and *Pseudomonas syringae*. Mol. Microbiol. **40:**1129–1139.
38. **Kaneko, T., Y. Nakamura, S. Sato, E. Asamizu, T. Kato, S. Sasamoto, A. Watanabe, K. Idesawa, A. Ishikawa, K. Kawashima, T. Kimura, Y. Kishida, C. Kiyokawa, M. Kohara, M. Matsumoto, A. Matsuno, Y. Mochizuki, S. Nakayama, N. Nakazaki, S. Shimpo, M. Sugimoto, C. Takeuchi, M. Yamada, and S. Tabata.** 2000. Complete genome structure of the nitrogen-fixing symbiotic bacterium *Mesorhizobium loti*. DNA Res. **7:**331–338.
39. **Keen, N. T.** 1990. Gene-for-gene complementarity in plant-pathogen interactions. Annu. Rev. Genet. **24:**447–463.
40. **Kim, J. G., E. Jeon, J. Oh, J. S. Moon, and I. Hwang.** 2004. Mutational analysis of *Xanthomonas* harpin HpaG identifies a key functional region that elicits the hypersensitive response in nonhost plants. J. Bacteriol. **186:**6239–6247.
41. **Kim, J. G., B. K. Park, C. H. Yoo, E. Jeon, J. Oh, and I. Hwang.** 2003. Characterization of the *Xanthomonas axonopodis* pv. *glycines* Hrp pathogenicity island. J. Bacteriol. **185:**3155–3166.
42. **Krishnan, H. B.** 2002. NopX of *Sinorhizobium fredii* USDA257, a type III-secreted protein involved in host range determination, is localized in the infection threads of cowpea (*Vigna unguiculata* [L.] Walp) and soybean (*Glycine max* [L.] Merr.) nodules. J. Bacteriol. **184:**831–839.
43. **Krishnan, H. B., J. Lorio, W. S. Kim, G. Jiang, K. Y. Kim, M. DeBoer, and S. G. Pueppke.** 2003. Extracellular proteins involved in soybean cultivar-specific nodulation are associated with pilus-like surface appendages and exported by a type III protein secretion system in *Sinorhizobium* USDA257. Mol. Plant-Microbe Interact. **16:**617–625.
44. **Krishnan, H. B., and S. G. Pueppke.** 1993. Flavonoid inducers of nodulation genes stimulate *Rhizobium fredii* USDA257 to export proteins into the environment. Mol. Plant-Microbe Interact. **6:**107–113.
45. **Laemmli, U. K.** 1970. Cleavage of structural proteins during the assembly of the head of bacteriophage T4. Nature **227:**680–685.
46. **Lavie, M., E. Shillington, C. Eguiluz, N. Grimsley, and C. Boucher.** 2002. PopP1, a new member of the YopJ/AvrRxv family of type III effector proteins, acts as a host-specificity factor and modulates aggressiveness of *Ralstonia solanacearum*. Mol. Plant-Microbe Interact. **15:**1058–1068.
47. **Lee, B. M., Y. J. Park, D. S. Park, H. W. Kang, J. G. Kim, E. S. Song, I. C. Park, U. H. Yoon, J. H. Hahn, B. S. Koo, G. B. Lee, H. Kim, H. S. Park, K. O. Yoon, J. H. Kim, C. H. Jung, N. H. Koh, J. S. Seo, and S. J. Go.** 2005. The genome sequence of *Xanthomonas oryzae* pathovar *oryzae* KACC10331, the bacterial blight pathogen of rice. Nucleic Acids Res. **33:**577–586.
48. **Lee, J., B. Klusener, G. Tsiamis, C. Stevens, C. Neyt, A. P. Tampakaki, N. J. Panopoulos, J. Noller, E. W. Weiler, G. R. Cornelis, J. W. Mansfield, and T. Nurnberger.** 2001. HrpZ(Psph) from the plant pathogen *Pseudomonas syringae pv. phaseolicola* binds to lipid bilayers and forms an ion-conducting pore *in vitro*. Proc. Natl. Acad. Sci. USA **98:**289–294.
49. **Li, C. M., I. Brown, J. Mansfield, C. Stevens, T. Boureau, M. Romantschuk, and S. Taira.** 2002. The Hrp pilus of *Pseudomonas syringae* elongates from its tip and acts as a conduit for translocation of the effector protein HrpZ. EMBO J. **21:**1909–1915.
50. **Marenda, M., B. Brito, D. Callard, S. Genin, P. Barberis, C. Boucher, and M. Arlat.** 1998. PrhA controls a novel regulatory pathway required for the specific induction of *Ralstonia solanacearum hrp* genes in the presence of plant cells. Mol. Microbiol. **27:**437–453.
51. **Marie, C., W. J. Deakin, V. Viprey, J. Kopcinska, W. Golinowski, H. B. Krishnan, X. Perret, and W. J. Broughton.** 2003. Characterization of Nops, nodulation outer proteins, secreted via the type III secretion system of NGR234. Mol. Plant-Microbe Interact. **16:**743–751.
52. **Neyt, C., and G. R. Cornelis.** 1999. Insertion of a Yop translocation pore into the macrophage plasma membrane by *Yersinia enterocolitica*: requirement for translocators YopB and YopD, but not LcrG. Mol. Microbiol. **33:**971–981.
53. **Nimchuk, Z., T. Eulgem, B. F. Holt III, and J. L. Dangl.** 2003. Recognition and response in the plant immune system. Annu. Rev. Genet. **37:**579–609.
54. **Noel, L., F. Thieme, D. Nennstiel, and U. Bonas.** 2002. Two novel type III-secreted proteins of *Xanthomonas campestris* pv. *vesicatoria* are encoded within the *hrp* pathogenicity island. J. Bacteriol. **184:**1340–1348.
55. **Occhialini, A., S. Cunnac, N. Reymond, S. Genin, and C. Boucher.** 2005. Genome-wide analysis of gene expression in *Ralstonia solanacearum* reveals that the hrpB gene acts as a regulatory switch controlling multiple virulence pathways. Mol. Plant-Microbe Interact. **18:**938–949.
56. **Petnicki-Ocwieja, T., K. van Dijk, and J. R. Alfano.** 2005. The *hrpK* operon of *Pseudomonas syringae* pv. *tomato* DC3000 encodes two proteins secreted by the type III (Hrp) protein secretion system: HopB1 and HrpK, a putative type III translocator. J. Bacteriol. **187:**649–663.
57. **Prentki, P., and H. M. Krisch.** 1984. *In vitro* insertional mutagenesis with a selectable DNA fragment. Gene **29:**303–313.
58. **Puhler, A., M. Arlat, A. Becker, M. Gottfert, J. P. Morrissey, and F. O'Gara.** 2004. What can bacterial genome research teach us about bacteria-plant interactions? Curr. Opin. Plant Biol. **7:**137–147.
59. **Roine, E., W. Wei, J. Yuan, E. L. Nurmiaho-Lassila, N. Kalkkinen, M. Romantschuk, and S. Y. He.** 1997. Hrp pilus: an *hrp*-dependent bacterial surface appendage produced by *Pseudomonas syringae pv. tomato* DC3000. Proc. Natl. Acad. Sci. USA **94:**3459–3464.
60. **Romantschuk, M., E. Roine, and S. Taira.** 2001. Hrp pilus - reaching through the plant cell wall. Eur. J. Plant Pathol. **107:**153–160.
61. **Rossier, O., G. Van den Ackerveken, and U. Bonas.** 2000. HrpB2 and HrpF from *Xanthomonas* are type III-secreted proteins and essential for pathogenicity and recognition by the host plant. Mol. Microbiol. **38:**828–838.
62. **Ryndak, M. B., H. Chung, E. London, and J. B. Bliska.** 2005. Role of predicted transmembrane domains for type III translocation, pore formation, and signaling by the *Yersinia pseudotuberculosis* YopB protein. Infect. Immun. **73:**2433–2443.
63. **Saad, M. M., H. Kobayashi, C. Marie, I. R. Brown, J. W. Mansfield, W. J. Broughton, and W. J. Deakin.** 2005. NopB, a type III secreted protein of *Rhizobium* sp. strain NGR234, is associated with pilus-like surface appendages. J. Bacteriol. **187:**1173–1181.
64. **Salanoubat, M., S. Genin, F. Artiguenave, J. Gouzy, S. Mangenot, M. Arlat, A. Billault, P. Brottier, J. C. Camus, L. Cattolico, M. Chandler, N. Choisne, C. Claudel-Renard, S. Cunnac, N. Demange, C. Gaspin, M. Lavie, A. Moisan, C. Robert, W. Saurin, T. Schiex, P. Siguier, P. Thebault, M. Whalen, P. Wincker, M. Levy, J. Weissenbach, and C. A. Boucher.** 2002. Genome sequence of the plant pathogen *Ralstonia solanacearum*. Nature **415:**497–502.
65. **Sarker, M. R., C. Neyt, I. Stainier, and G. R. Cornelis.** 1998. The *Yersinia* Yop virulon: LcrV is required for extrusion of the translocators YopB and YopD. J. Bacteriol. **180:**1207–1214.
66. **Schechter, L. M., K. A. Roberts, Y. Jamir, J. R. Alfano, and A. Collmer.** 2004. *Pseudomonas syringae* type III secretion system targeting signals and novel effectors studied with a Cya translocation reporter. J. Bacteriol. **186:**543–555.
67. **Sory, M. P., and G. R. Cornelis.** 1994. Translocation of a hybrid YopE-adenylate cyclase from *Yersinia enterocolitica* into HeLa cells. Mol. Microbiol. **14:**583–594.
68. **Sugio, A., B. Yang, and F. F. White.** 2005. Characterization of the hrpF pathogenicity peninsula of *Xanthomonas oryzae pv. oryzae*. Mol. Plant-Microbe Interact. **18:**546–554.
69. **Szurek, B., O. Rossier, G. Hause, and U. Bonas.** 2002. Type III-dependent translocation of the *Xanthomonas* AvrBs3 protein into the plant cell. Mol. Microbiol. **46:**13–23.
70. **Tardy, F., F. Homble, C. Neyt, R. Wattiez, G. R. Cornelis, J. M. Ruysschaert, and V. Cabiaux.** 1999. *Yersinia enterocolitica* type III secretion-translocation system: channel formation by secreted Yops. EMBO J. **18:**6793–6799.
71. **Thompson, J. D., T. J. Gibson, F. Plewniak, F. Jeanmougin, and D. G. Higgins.** 1997. The CLUSTAL_X windows interface: flexible strategies for multiple sequence alignment aided by quality analysis tools. Nucleic Acids Res. **25:**4876–4882.
72. **Thompson, J. D., D. G. Higgins, and T. J. Gibson.** 1994. CLUSTAL W: improving the sensitivity of progressive multiple sequence alignment through sequence weighting, position-specific gap penalties and weight matrix choice. Nucleic Acids Res. **22:**4673–4680.
73. **Turner, P., C. Barber, and M. Daniels.** 1984. Behavior of the transposons Tn5 and Tn7 in *Xanthomonas campestris pv. campestris*. Mol. Gen. Genet. **195:**101–107.
74. **Van Gijsegem, F., J. Vasse, J. C. Camus, M. Marenda, and C. Boucher.** 2000. *Ralstonia solanacearum* produces hrp-dependent pili that are required for PopA secretion but not for attachment of bacteria to plant cells. Mol. Microbiol. **36:**249–260.
75. **Van Gijsegem, F., J. Vasse, R. De Rycke, P. Castello, and C. Boucher.** 2002. Genetic dissection of *Ralstonia solanacearum* hrp gene cluster reveals that the HrpV and HrpX proteins are required for Hrp pilus assembly. Mol. Microbiol. **44:**935–946.
76. **Weber, E., T. Ojanen-Reuhs, E. Huguet, G. Hause, M. Romantschuk, T. K. Korhonen, U. Bonas, and R. Koebnik.** 2005. The type III-dependent Hrp pilus is required for productive interaction of *Xanthomonas campestris* pv. *vesicatoria* with pepper host plants. J. Bacteriol. **187:**2458–2468.
77. **Yu, H. B., P. S. Rao, H. C. Lee, S. Vilches, S. Merino, J. M. Tomas, and K. Y. Leung.** 2004. A type III secretion system is required for *Aeromonas hydrophila* AH-1 pathogenesis. Infect. Immun. **72:**1248–1256.
78. **Zhu, W., M. M. MaGbanua, and F. F. White.** 2000. Identification of two novel hrp-associated genes in the *hrp* gene cluster of *Xanthomonas oryzae* pv. *oryzae*. J. Bacteriol. **182:**1844–1853.